15. Plumier JC, Ross BM, Currie RW, et al. Transgenic mice expressing the human heat shock protein 70 have improved post-ischemic myocardial recovery. *J Clin Invest.* 1995;95:1854–1860.
16. Marber MS, Mestril R, Chi SH, et al. Overexpression of the rat inducible 70-kD heat stress protein in a transgenic mouse increases the resistance of the heart to ischemic injury. *J Clin Invest.* 1995;95:1446–1456.
17. Radford NB, Fina M, Benjamin IJ, et al. Cardioprotective effects of 70-kDa heat shock protein in transgenic mice. *Proc Natl Acad Sci U S A.* 1996;93:2339–2342.
18. Figueras J, Segura R, Bermejo B. Repeated 15-minute coronary occlusions in pigs increase occlusion arrhythmias but decrease reperfusion arrhythmias that are associated with extracellular hypokalemia. *J Am Coll Cardiol.* 1996;28:1589–1597.
19. Saleh A, Srinivasula SM, Balkir L, et al. Negative regulation of the Apaf-1 apoptosome by Hsp70. *Nat Cell Biol.* 2000;2:476–483.
20. Pandey P, Saleh A, Nakazawa A, et al. Negative regulation of cytochrome c-mediated oligomerization of Apaf-1 and activation of procaspase-9 by heat shock protein 90. *EMBO J.* 2000;19:4310–4322.
21. Condorelli G, Roncarati R, Ross JJ, et al. Heart-targeted overexpression of caspase3 in mice increases infarct size and depresses cardiac function. *Proc Natl Acad Sci U S A.* 2001;98:9977–9982.
22. Okamura T, Miura T, Takemura G, et al. Effect of caspase inhibitors on myocardial infarct size and myocyte DNA fragmentation in the ischemia-reperfused rat heart. *Cardiovasc Res.* 2000;45:642–650.
23. Mockridge JW, Marber MS, Heads RJ. Activation of Akt during simulated ischemia/reperfusion in cardiac myocytes. *Biochem Biophys Res Commun.* 2000;270:947–952.
24. He H, Li HL, Lin A, et al. Activation of the JNK pathway is important for cardiomyocyte death in response to simulated ischemia. *Cell Death Differ.* 1999;6:987–991.
25. Pham FH, Sugden PH, Clerk A. Regulation of protein kinase B and 4E-BP1 by oxidative stress in cardiac myocytes. *Circ Res.* 2000;86:1252–1258.
26. Matsui T, Tao J, del MF, et al. Akt activation preserves cardiac function and prevents injury after transient cardiac ischemia in vivo. *Circulation.* 2001;104:330–335.
27. Hreniuk D, Garay M, Gaarde W, et al. Inhibition of c-Jun N-terminal kinase 1, but not c-Jun N-terminal kinase 2, suppresses apoptosis induced by ischemia/reoxygenation in rat cardiac myocytes. *Mol Pharmacol.* 2001;59:867–874.
28. Sato S, Fujita N, Tsuruo T. Modulation of Akt kinase activity by binding to Hsp90. *Proc Natl Acad Sci U S A.* 2000;97:10832–10837.
29. Brouet A, Sonveaux P, Dessy C, et al. Hsp90 and caveolin are key targets for the proangiogenic nitric oxide-mediated effects of statins. *Circ Res.* 2001;89:866–873.
30. Park HS, Lee JS, Huh SH, et al. Hsp72 functions as a natural inhibitory protein of c-Jun N-terminal kinase. *EMBO J.* 2001;20:446–456.

Human Molecular Genetics, 2003, Vol. 12, No. 6 **595–600**
DOI: 10.1093/hmg/ddg065

cDNA microarray analysis of individual Duchenne muscular dystrophy patients

Satoru Noguchi[1,2], Toshifumi Tsukahara[1,*], Masako Fujita[1,2], Rumi Kurokawa[1,2], Masaji Tachikawa[2,3], Tatsushi Toda[2,3], Atsumi Tsujimoto[2,4], Kiichi Arahata[1,2,†] and Ichizo Nishino[1,2]

[1]Department of Neuromuscular Research, National Institute of Neuroscience, National Center of Neurology and Psychiatry, 4-1-1 Ogawahigashi, Kodaira, Tokyo 187-8502, Japan, [2]Core Research for Evolutional Science and Technology (CREST), Japan Science and Technology Corporation, Kawaguchi, Saitama 332-0012, Japan, [3]Division of Functional Genomics, Department of Post-Genomics and Diseases, Osaka University Graduate School of Medicine, Suita, Osaka 565-0871, Japan and [4]DNA Chip Research Inc, Yokohama, Kanagawa 230-0045, Japan

Received October 1, 2002; Revised and Accepted January 17, 2003

We have developed a novel cDNA microarray encompassing 3500 genes expressed in skeletal muscle. With this system, we have performed the first study of gene expression in samples from individual patients. We analyzed muscle specimen from individuals with Duchenne muscular dystrophy to identify differences among patients. Among the variably expressed genes, we focused on the expression of the genes encoding HLA-related proteins, myosin light chains and troponin Ts as markers of muscle necrosis and regeneration. The expression patterns of these genes correlated with the severity of dystrophic changes on histological examination. Our cDNA microarray provides a new tool to investigate molecular muscle pathology.

INTRODUCTION

Dystrophin gene mutations cause dystrophin deficiency in sarcolemma giving rise to Duchenne muscular dystrophy (DMD) (1). Dystrophin is associated with several sarcolemmal proteins that connect the cytoskeleton and extracellular matrix (2). This connection bolsters the mechanical strength of the sarcolemma against muscle contraction-induced tension (3). In muscle lacking dystrophin, the connection is weakened and sarcolemma is exposed to high tension. It causes partial disruptions of sarcolemma leading to an influx of extracellular Ca^{2+}. The elevation of intracellular Ca^{2+} concentration activates the calcium-dependent degradative pathway resulting in myofibril disruption and muscle necrosis (4). However, this mechanism has not been proven definitively.

It has been postulated that dystrophin is involved in signal transduction, because dystrophin has multiple phosphorylation sites and the dystrophin-associated proteins bind to Grb2, ERK6 and nNOS (5–7). Moreover, DMD muscles also show hypertrophy in some myofibers. To account for this muscle hypertrophy, two possible mechanisms have been proposed: abnormal IGF-1 and GDF8-mediated signal pathways (8,9). To clarify the mechanisms causing dystrophic changes and muscle hypertrophy in DMD, it is necessary to understand the molecular events that occur in dystrophic muscle. cDNA microarray/gene chip analyses provide comprehensive quantitative assays for transcripts and have been broadly applied to assess alterations of gene expression in diseases (10).

DMD and α-sarcoglycanopathy have been analyzed by cDNA microarray/gene chip technique. The data clearly reveal expression profiles that are characteristic of DMD and α-sarcoglycanopathy (11,12). However, these analyses have several limitations: (1) the cDNA probes plotted on the microarrays do not cover all of the genes expressed in skeletal muscle; (2) the properties of probe cDNAs have not been not well-characterized; (3) homologous genes of each target gene may cross-hybridize with the probes; and (4) because relatively large amounts of RNA are required, each microarray analysis has required pooled RNA samples from several patients (11). To resolve these problems, we developed a novel high-quality cDNA microarray and devised an analytical method. We applied our array to study gene expression in individual DMD patients in order to identify specific transcriptional changes related to the pathophysiological alterations in each patient.

*To whom correspondence should be addressed. Tel: +81 423412712; Fax: +81 423461742; Email: tukahara@ncnp.go.jp
†Deceased.

RESULTS

Generation of a cDNA array collecting skeletal muscle transcripts

To generate novel cDNA microarray, we initially collected information about all genes related to skeletal muscle available through public databases. Based upon these data, we designed cDNAs probes. Blast searches were performed with each candidate probe to exclude the possibility of cross-hybridization with homologous genes. We identified cDNA fragments of 450–550 bp in size to minimize cross-hybridization. We made a cDNA microarray contained more than 4224 cDNA probes representing 3500 genes. This array showed significant reproducibility with a high correlation factor (>0.984), when target cDNAs, prepared from 1 μg of total RNA, were repeatedly hybridized. The hybridization spot intensities showed linearities of targets over a range that exceeded three-logs with 0.5–4 μg of total RNA (not shown).

cDNA microarray analysis with RNA from individual biopsy specimen

Histopathological features were assessed in each patient, because the severity of dystrophic phenotype differed among the patients. Because of the pathological variability, we thought that the expression analyses with the cDNA microarray should be performed on individual patients. Therefore, we developed methods to isolate and quantitate total RNA from small biopsy specimens and employed an enhanced detection system using tyramide signal amplification. Our microarray system first enabled us to analyze a gene expression profile in only 10–30 mg of frozen muscle and thus study a sample from a single patient. To confirm the reliability of our cDNA microarray, we analyzed the expression levels of whole transcripts in normal skeletal muscle. The cDNA probes were ordered according to their mean hybridized intensities in duplicate analyses. Probes derived from the same genes showed similar intensities. The ranking of genes matched well with those of EST abundance reported by Bortoluzzi *et al.* (13) and BODYMAP (14), thus demonstrating compatibility of our data with those with other methods. The ranking of genes expressed in skeletal muscle and its comparison are presented in supplemental data (Supplementary Table 1).

The common features of gene expression in DMD muscles

In this study, cDNA microarray analyses were carried out by competitive hybridization using probes from individual DMD and normal muscles, and the ratio of the both probe (signal intensitiy in DMD/signal intensitiy in control) in each experiment were estimated as differences in gene expression levels. We collected the data from the muscles of six patients and the complete sets of data are presented in Supplementary Table 2. To characterize the common features of gene expression in DMD muscles, average ratios for each spot in the six patients were calculated. Of the 3500 genes assessed by 4224 probes, 77 genes showed more than 2-fold increased expression in DMD muscle compared to controls, while 343 genes revealed decreased expression (less than 50% of controls) (Fig. 1). Table 1 shows the distribution of these upregulated and downregulated genes by functional classification. The complete sets of the variable genes are listed in supplementary data (Supplementary Tables 3 and 4). Genes related to immune response, sarcomere, extracellular matrix (ECM) and signaling/cell growth were increased predominantly. Most of the increased immune response-related genes are HLA-DR genes of major histocompatibility complex classes I and II, which are expressed in antigen-presenting cells. Upregulated sarcomere-related genes are α-cardiac actin, myosin light chain (MYL) 4 and 1, and myosin binding protein H genes, which are known to be expressed developmentally in fetal muscles (15). Increased ECM genes are type III collagen α-1, type XV collagen α-1, SPARC and thrombospondin-4 genes. Upregulation of these genes reflect dystrophic changes in DMD muscles such as myofiber necrosis, inflammation and muscle regeneration. In contrast, genes involved in energy metabolism, transcription/translation, signaling and proteasomes were downregulated (Table 2). The genes in energy metabolism encode several enzymes involved in glycolytic pathway and electron transfer reactions in mitochondria (Supplementary Table 4). The genes in transcription/translation category encode transcriptional factors, initiation/elongation factors and ribosomal proteins, which are closely related to protein synthesis. Thus, downregulation of these genes may reflect the chronic decline in muscle function and homeostasis. Furthermore, our study revealed additional interesting findings. Genes encoding sarcomeric proteins were involved in both upregulated and downregulated groups. Interestingly, genes encoding skeletal and cardiac muscle actins and MYL 1, 3 and 4 isoforms, which are principal components in myofibrils, were strikingly upregulated. In contrast, genes encoding myofibril-associated or regulatory proteins, myosin-binding protein C, myomesin, titin, nebulin, desmin, telethonin and calpain 3 were downregulated. The genes expressed in slow fibers also tended to be downregulated.

Differences in gene expression in muscles among the patients

DMD is a progressive disorder and muscles from patients show a rather wide range of pathological changes depending on the stage of the illness. We monitored these pathological changes by histological examination of muscle sections from the patients (Fig. 2). The muscles from patients 4, 5 and 6 showed marked muscle fiber necrosis (asterisks) and regeneration (arrowheads) in addition to variations in fiber size and endomysial fibrosis (see also Table 1). In contrast, samples from patients 1, 2 and 3 showed much milder changes and these changes are least prominent in patients 2 and 3. We studied the difference in gene expression among the patients. Differences in gene expression in muscles among the patients should reflect the difference in the pathophysiological changes. Figure 3 shows the expression pattern of all probes in six patients in microarray analyses by Gene spring software from the data presented in Supplementary Table 2. Each of the horizontal color lines denotes the expression difference in each probe showing the upregulation in red or the downregulation in blue. All patients generally showed similar gene expression patterns, but in some probes the differences among the patients were remarkable. This

Table 1. Clinicopathological features of the patients

Patient	Age at biopsy	Learned to walk	Muscle atrophy	Gowers sign[a]	Waddling gait	CK level (IU/l)	Necrotic fibers (%)	Regenerating fibers (%)
1	3 years 3 months	1 year 2 months	None	Mild	Mild	18 617	0.3	3
2	1 year	1 year 1 month	None	Minimal	Minimal	20 994	0.2	2
3	1 year 6 months	1 year 3 months	Minimal	Minimal	None	24 360	0.2	2
4	1 year 10 months	1 year 9 months	None	Minimal	None	19 450	0.3	5
5	5 years	2 years 1 month	Mild	Typical	Typical	14 153	0.5	4
6	4 years	1 year 6 months	Mild	Typical	Typical	21 839	0.5	5

[a]Gowers sign was evaluated as follows; minimal, hip is first raised when standing up; mild, hands are mildly put on the knees; typical, with efforts.

Table 2. Classification of the genes representing variable expression more than 2-fold or less than 1/2-fold

Category	Number of genes with increased expression	Number of genes with decreased expression
Energy metabolism	0	53
Transcription/translation	1	45
Signal/cell growth	5	39
Sarcomere	8	24
Enzyme	7	24
Cytoskeleton	6	15
Receptor/channel	2	14
Immune response	11	2
Proteasome	1	10
ECM	9	1
Chaperone	0	8
Others	11	16
Unknown	16	76
Total	77	327

experimental tree classified the patients into two groups, one consisting of patients 4, 5, and 6, and another containing patients 1, 2, and 3. This classification is essentially in accordance with the observation in histological examination in Figure 2 and Table 1.

We hypothesized that the changes in expression of some genes reflect the state of pathological process in the patients' muscles. Therefore, we focused on genes related to the muscle necrosis and regeneration. As markers for muscle necrosis, we selected *HLA-related* genes, *TIMP3* and C-X-C chemokine *Scyb14* genes, which are known to be expressed in the infiltrating cells, dendritic cells or lymphocytes during immune response (16). We found that the expression level of these genes differed among the patients as shown in Figure 4A. These genes were strongly upregulated in patients 1, 4, 5 and 6, as indicated by red colors, while they were normally expressed in patients 2 and 3. These results indicate that patients 1, 4, 5, and 6 have more severe necrotic changes than patients 2 and 3, and are in accordance with the histological results shown in Figure 2. This observation was also confirmed by the differential expression of basic FGF, another marker for muscle degeneration among these patients (data not shown) (17).

We further hypothesized that regenerating process in muscle fibers will reproduce the course of expression of developmentally activated genes. We observed that several genes encoding muscle proteins, such as myosin heavy chains, MYLs, tropomyosin, myosin binding protein H, troponins, muscle creatine kinase, and myoglobin, showed the differential expression among patients (15). Among these genes, we found two gene families, *MYL* and *troponin T* (*TNNT*) which showed clear differences in expression between patients but also showed the distinct expression patterns between their gene isoforms. Figure 4B shows the expression levels of *MYL* gene family among six patients. In patients 5 and 6 with intensive muscle regeneration on histological examination, all *MYL* isoform genes were strongly expressed as shown in red signals. In patients 1, 2 and 3, *MYL4*, *MYL1* and *MYL3* genes were mildly upregulated as demonstrated in yellow to red signals; however, *MYL2* was expressed much less in patients than in controls as indicated by in blue signals. Similarly, Figure 4C shows the expression levels of *TNNT* gene family among six patients. Patients 5 and 6 showed significant upregulation of all *TNNT* genes, and patient 4 showed slight expression of *TNNT2* and *TNNT3*, while patients 1, 2 and 3 showed only faint expression in *TNNT2* as shown in gray. We also confirmed the differential expression of marker proteins for regeneration, NCAM and myogenin (18) among these patients (data not shown). Overall, our results suggest that transcripts from three groups of genes, HLA-related, *MYL* and *TNNT* are useful reporters for monitoring dystrophic changes at the molecular level.

DISCUSSION

With our novel microarray, we performed the first gene expression studies in muscle samples from individual patients. The analysis of DMD muscles from individual patients provided information about gene expression profile not only to deduce common pathognomonic features but also to highlight differences among patients at the molecular level. In common pathognomonic features in gene expression alteration, we found that developmentally expressed genes were significantly upregulated while the genes related to muscle homeostasis were downregulated. These changes reflect various cellular events including muscle necrosis and regeneration. These up- and downregulated genes are compatible with the results by Chen *et al.* (11) and Tkatchenko *et al.* (12). In addition, genes encoding principal components in myofibrils were strikingly upregulated while genes encoding myofibril-associated or regulatory proteins were downregulated, suggesting that these gene groups might be regulated by different mechanism, although only limited information is available about the promoters of some genes in these groups. We found that the genes expressed in slow-type fiber were also

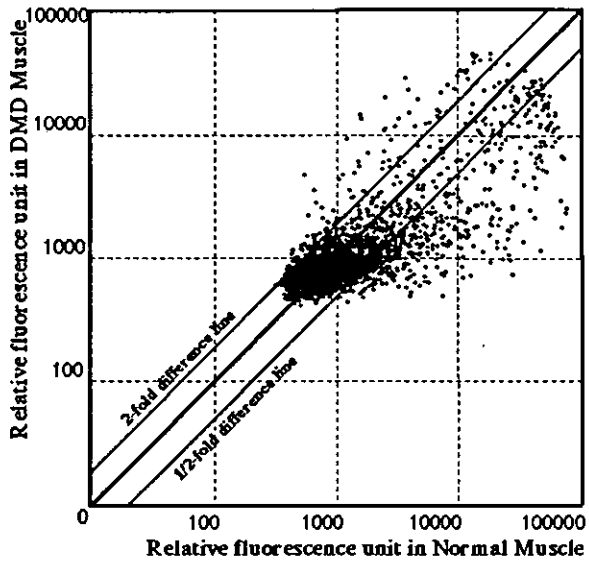

Figure 1. Scatter plot of the average expression intensities on all spots between DMD patients and control. The diagonal line shows similar expression between DMD patients and control. The lines showing the 2-fold and 1/2-fold differences also indicated; 90.5% of probes present between the two lines.

downregulated. The downregulation of these genes accompanied with the downregulation of mitochondrial energy metabolic genes in DMD muscles. This finding is interesting on the relation with recent report in which the activation of transcriptional complexes containing of PGC-1 in contractile stimulation upregulates the slow-type fiber genes and mitochondrial energy metabolic genes (19).

We have demonstrated the expression of genes related to muscle necrosis and regeneration among the patients. We detected the upregulation of HLA-related genes, *TIMP3* and *C-X-C chemokine Scyb14* genes dependent on the severity of necrotic changes in each patient's muscle. Their differential expression would indicate the degree of infiltration, activation of monocytes and lymphocytes and inflammatory response in necrotic areas of muscle among the patients (16). As muscle regeneration markers, we found the differential upregulation of *MYL* and *TNNT* isoform genes among patients dependent on the degrees of muscle regeneration in DMD muscle fibers. Progressive expression of each isoform in these families during mouse skeletal muscle development has also been reported (20). In the *MYL* gene family, *MYL4* gene is activated initially, followed by sequential activation of the *MYL1* and *MYL3* genes during embryonic stages, while *MYL2* is only expressed after birth (21). In the *TNNT* gene family, *TNNT2* is expressed initially, and later *TNNT3* and *TNNT1* are expressed during mouse skeletal muscle development (22). The differential upregulation of *MYL* and *TNNT* gene isofoms among patients were well-matched with the progression of the muscle regenerating process, and reproduced the developmental expression patterns of these genes. Our data suggest that slow type genes, *MYL2* and *TNNT1* are the most sensitive marker of muscle fiber regeneration.

Our microarray data are in accordance with the histological abnormalities suggesting that this system may be used to monitor pathological changes in dystrophic muscles. Since our microarray requires only a small amount of muscle tissue, this system might contribute to providing additional information to histological analyses for the diagnosis and the evaluation of the muscular diseases, especially those with patchy necrotic and regenerating lesions, such as polymyositis in which multiple punch biopsies would help to make a diagnosis. Comprehensive gene expression analysis will also provide valuable information about mechanisms of muscle degeneration, degrees of progression or interruption of muscle regeneration, and differences at the molecular level among patients and among diseases. Our cDNA microarray will open a door to a new molecular pathology in the field of myology.

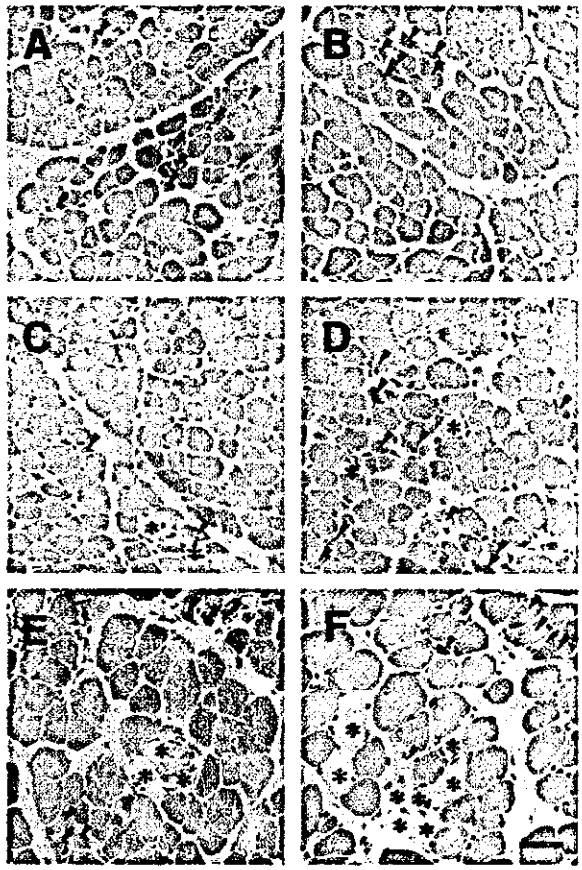

Figure 2. Histological staining of skeletal muscle from DMD patients. Muscle sections show different degrees of dystrophic changes with variable muscle necrosis (asterisks) and regeneration (arrowheads) by hematoxylin and eosin staining. Bar indicates 100 μm. (**A**) patient 1, (**B**) patient 2, (**C**) patient 3, (**D**) patient 4, (**E**) patient 5 and (**F**) patient 6.

MATERIALS AND METHODS

Construction of the cDNA microarray

By database searches, we selected genes computationally including ESTs expressed in skeletal muscle and constructed

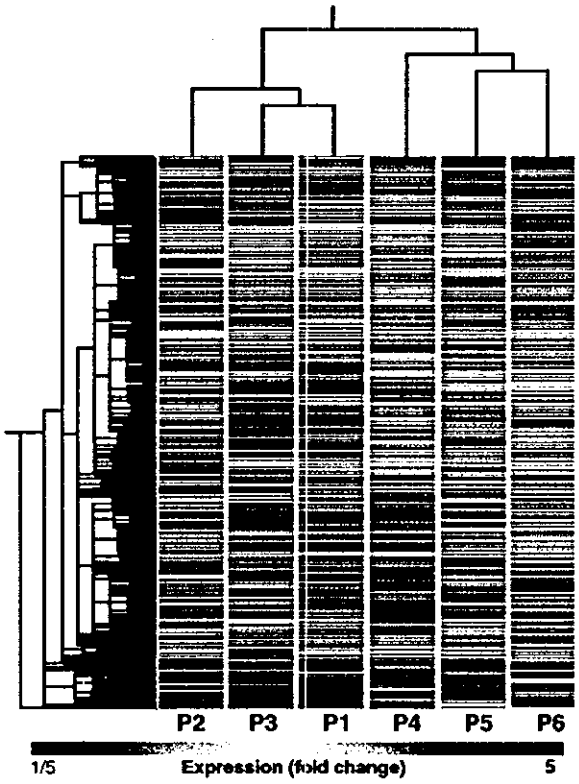

Figure 3. cDNA microarray analyses of skeletal muscle of DMD patients. Differences in gene expression are shown in color as bottom scale (5-fold expression in red to 1/5-fold expression in blue). The data for each patient are shown in each vertical column with an experimental tree. The probes were classified and aligned based on the expression differences in all patients as shown in left tree. P1, patient 1; P2, patient 2; P3, patient 3; P4, patient 4; P5, patient 5; P6, patient 6.

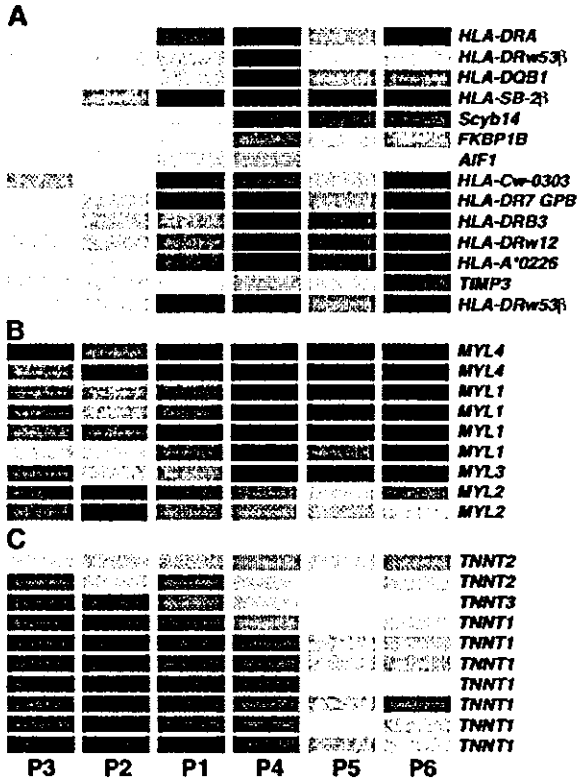

Figure 4. Differential expression of HLA-related, MYL and TNNT genes in skeletal muscle of DMD patients. (A) The expression differences in probes with HLA-related genes. (B) Probes with *MYL* family genes. (C) Probes with *TNNT* family genes. The data are represented as in Figure 3. P1, patient 1; P2, patient 2; P3, patient 3; P4, patient 4; P5, patient 5; P6, patient 6.

probes for each predicted gene using the overlapping sequence. For each singleton, we designed one or more probes with unique sequence with lengths of 450–550 bp in the vicinity of 3′-ends of each transcript in order to obtain almost same hybridized condition for all spots and to minimize the possible cross-hybridization to other genes. We amplified cDNA fragments using specific primer pairs and cloned the PCR products into a pCR/blunt vector (Invitrogen, Carlsbad, CA, USA). All cloned products were confirmed by cycle sequencing on ABI prism 3100 (Applied Biosystems, Foster City, CA, USA). The inserts were amplified as probes with vector-arm primers, normalized in amounts and spotted on slideglass precoated with poly-L-lysine.

Preparation of total RNA from skeletal muscle biopsy specimens

Informed consent was obtained from all subjects. All patients used in this study were clinicopathologically diagnosed as DMD and all of their muscles showed no dystrophin-staining. The clinicopathological features of the patients are listed in Table 1. Muscle biopsy was carried on from biceps brachii muscles at ages as follows: patient 1, 3 years; patient 2, 1 year; patient 3, 1 year 6 months; patient 4, 1 year 10 months; patient 5, 5 years; patient 6, 4 years. We prepared total RNA from the 50–100 cryosections (6 μm thickness) of each muscle biopsy specimen with Cyto-plasmic RNA reagent (Invitrogen) according to the manufacturer's protocol. The amounts of total RNA were estimated by semi-quantitative RT–PCR with an intron-spanning primer pair for muscle creatine kinase coding region using the following used primer sets 5′-TTCATGTGGAACCAACACC-3′ (811–829) and 5′-CAGAATCCAGAGGATGGAGC-3′ (1334–1315). The amplified products from stepwise-diluted sample were compared with those from stepwise-diluted standard RNA from normal muscle.

Histological examination of skeletal muscle specimens

Hematoxylin and eosin staining and immunohistochemical staining of cryosections of biopsy specimens from patient skeletal muscles were performed by standard method.

Microarray analyses

The production of labeled cDNA targets, hybridization and detection on microarray were performed with TSA Labeling

and Detection Kit (Perkin-Elmer Life Science, Boston, MA, USA) according to the manufacturer's protocol. We used approximately 1–2 μg of total RNA for labeling and used aliquots of the labeled products corresponding to 1 μg of total RNA for hybridization. The microarray experiments were carried out by competitive hybridization using two labeled targets from DMD muscle and normal one. Patients 3, 4, 5 and 6 were analyzed in duplicate experiments and patients 1 and 2 were analyzed only in single experiments because of the limited amounts of specimens. The hybridized intensities on spots and the background intensities around spots were quantitated by ScanArray 5000 equipped with the software of ScanArray and QuantArray (Perkin-Elmer Life Science). Difference in gene expression was represented as ratio of the fluorescent intensity with DMD target to that of normal control target on each spot. The data preparation and statistical analysis were carried out with Microsoft Excel (Microsoft, Redmond, WA, USA) and Genespring (Silicon Genetics, Redwood City, CA, USA). The mean intensity (x) and standard deviation (σ) of the non-spotted areas without probes were calculated for each array, and the data of spots with the intensity value more than $x+5\sigma$ with at least one of two probes were used for statistical analyses. To deduce common features of gene expression in DMD muscles, we calculated the average ratio of each probe in all six patients' data and ranked the all genes according to these ratios using a median value if muliple probes from one gene were present. To compare expression profiling among DMD patients, we classified all probes using the ratio values in all patients' data with standard correlation at separation ratio 0.5 and minimum distance 0.001 by Gene tree classification and also classified the patients using all data by experimental tree classification in Genespring software.

SUPPLEMENTARY MATERIAL

Supplementary Material is available at HMG Online.

ACKNOWLEDGEMENTS

The authors thank Drs Y.K. Hayashi and I. Nonaka (National Center of Neurology and Psychiatry) for their critical comments and discussion on the manuscript, Dr M. Hirano (Columbia University) for reviewing the manuscript, Ms A. Nishiyama and S. Matsuno for their technical assistance.

REFERENCES

1. Koenig, M., Monaco, A.P. and Kunkel, L.M. (1988) The complete sequence of dystrophin predicts a rod-shaped cytoskeletal protein. *Cell*, **53**, 219–226.
2. Ozawa, E., Yoshida, M., Suzuki, A., Mizuno, Y., Hagiwara, Y. and Noguchi, S. (1995) Dystrophin-associated proteins in muscular dystrophy. *Hum. Mol. Genet.*, **4**, 1711–1716.
3. Petrof, B.J., Shrager, J.B., Stedman, H.H., Kelly, A.M. and Sweeney, H.L. (1993) Dystrophin protects the sarcolemma from stresses developed during muscle contraction. *Proc. Natl Acad. Sci. USA*, **90**, 3710–3714.
4. Turner, P.R., Schultz, R., Ganguly, B. and Steinhardt, R.A. (1993) Proteolysis results in altered leak channel kinetics and elevated free calcium in mdx muscle. *J. Membr. Biol.*, **133**, 243–251.
5. Michalak, M., Fu, S.Y., Milner, R.E., Busaan J.L. and Hance, J.E. (1996) Phosphorylation of the carboxyl-terminal region of dystrophin. *Biochem. Cell. Biol.*, **74**, 431–437.
6. Brenman, J.E., Chao, D.S., Xia, H., Aldape, K. and Bredt, D.S. (1995) Nitric oxide synthase complexed with dystrophin and absent from skeletal muscle sarcolemma in Duchenne muscular dystrophy. *Cell*, **82**, 743–752.
7. Hasegawa, M., Cuenda, A., Spillantini, M.G., Thomas, G.M., Buee-Scherrer, V., Cohen, P. and Goedert, M. (1999) Stress-activated protein kinase-3 interacts with the PDZ domain of alpha1-syntrophin. A mechanism for specific substrate recognition. *J. Biol. Chem.*, **274**, 12626–12631.
8. Musaro, A., McCullagh, K., Paul, A., Houghton, L., Dobrowolny, G., Molinaro, M., Barton, E.R., Sweeney, H.L. and Rosenthal, N. (2001) Localized Igf-1 transgene expression sustains hypertrophy and regeneration in senescent skeletal muscle. *Nat. Genet.*, **27**, 195–200.
9. McPherron, A.C., Lawler, A.M. and Lee, S.J. (1997) Regulation of skeletal muscle mass in mice by a new TGF-beta superfamily member. *Nature*, **387**, 83–90.
10. Greenberg, S.A. (2001) DNA microarray gene expression analysis technology and its application to neurological disorders. *Neurology*, **57**, 755–761.
11. Chen, Y.W., Zhao, P., Borup, R. and Hoffman, E.P. (2000) Expression profiling in the muscular dystrophies: identification of novel aspects of molecular pathophysiology. *J. Cell Biol.*, **151**, 1321–1336.
12. Tkatchenko, A.V., Pietu, G., Cros, N., Gannoun-Zaki, L., Auffray, C., Leger, J.J. and Dechesne, C.A. (2001) Identification of altered gene expression in skeletal muscles from Duchenne muscular dystrophy patients. *Neuromus. Disord.*, **11**, 269–277.
13. Bortoluzzi, S., d'Alessi, F., Romualdi, C. and Danieli, G.A. (2000) The human adult skeletal muscle transcriptional profile reconstructed by a novel computational approach. *Genome Res.*, **10**, 344–349.
14. Sese, J., Nikaidou, H., Kawamoto, S., Minesaki, Y., Morishita, S, Okubo K. (2001) BodyMap incorporated PCR-based expression profiling data and a gene ranking system. *Nucl. Acids Res.*, **29**, 156–158
15. Ontell, M., Ontell, M.P., Sopper, M.M., Mallonga, R., Lyons, G. and Buckingham, M. (1993) Contractile protein gene expression in primary myotubes of embryonic mouse hindlimb muscles. *Development*, **117**, 1435–1444.
16. Porter, J.D., Khanna, S., Kaminski, H.J., Rao, J.S., Merriam, A.P., Richmonds, C.R., Leahy, P., Li, J., Guo, W. and Andrade, F.H. (2002) A chronic inflammatory response dominates the skeletal muscle molecular signature in dystrophin-deficient mdx mice. *Hum. Mol. Genet.*, **11**, 263–272.
17. Anderson, J.E., Liu, L. and Kardami, E.V. (1991) Distinct patterns of basic fibroblast growth factor (bFGF) distribution in degenerating and regenerating areas of dystrophic (mdx) striated muscles. *Dev. Biol.*, **147**, 96–109.
18. Dedkov, E.I., Kostrominova, T.Y., Borisov, A.B. and Carlson, B.M. (2001) Reparative myogenesis in long-term denervated skeletal muscles of adult rats results in a reduction of the satellite cell population. *Anat. Rec.*, **263**, 139–154.
19. Lin, J., Wu, H., Tarr, P.T., Zhang, C.Y., Wu, Z., Boss, O., Michael, L.F., Puigserver, P., Isotani, E., Olson, E.N., Lowell, B.B. *et al.* (2002) Transcriptional co-activator PGC-1 alpha drives the formation of slow-twitch muscle fibers. *Nature*, **418**, 797–801.
20. Barton, P.J., Harris, A.J. and Buckingham, M.E. (1989) Myosin light chain gene expression in developing and denervated fetal muscle in the mouse. *Development*, **107**, 819–824.
21. Sutherland, C.J., Elsom, V.L., Gordon, M.L., Dunwoodie, S.L. and Hardeman, E.C. (1991) Coordination of skeletal muscle gene expression occurs late in mammalian development. *Dev. Biol.*, **146**, 167–178.
22. Wang, Q., Reiter, R.S., Huang, Q.Q., Jin, J.P. and Lin, J.J. (2001) Comparative studies on the expression patterns of three troponin T genes during mouse development. *Anat. Rec.*, **263**, 72–84.

Human Molecular Genetics, 2003, Vol. 12, No. 12 **1449–1459**
DOI: 10.1093/hmg/ddg153

Fukutin is required for maintenance of muscle integrity, cortical histiogenesis and normal eye development

Satoshi Takeda[1], Mari Kondo[1], Junko Sasaki[2], Hiroki Kurahashi[2], Hiroki Kano[2], Ken Arai[3], Kazuyo Misaki[4], Takehiko Fukui[5], Kazuhiro Kobayashi[2], Masaji Tachikawa[2], Michihiro Imamura[6], Yusuke Nakamura[7], Teruo Shimizu[3], Tatsufumi Murakami[8], Yoshihide Sunada[8], Takashi Fujikado[5], Kiichiro Matsumura[3], Toshio Terashima[4] and Tatsushi Toda[2,*]

[1]Otsuka GEN Research Institute, Otsuka Pharmaceutical Co. Ltd, Tokushima, Japan, [2]Division of Functional Genomics, Department of Post-Genomics and Diseases, Osaka University Graduate School of Medicine, 2-2-B9 Yamadaoka, Suita, Osaka 565-0871, Japan, [3]Department of Neurology, Teikyo University School of Medicine, Tokyo, Japan, [4]Department of Anatomy and Neurobiology, Kobe University Graduate School of Medicine, Kobe, Japan, [5]Department of Ophthalmology and Visual Science, Osaka University Graduate School of Medicine, Osaka, Japan, [6]Institute of Neuroscience, National Center for Neurology and Psychiatry, Tokyo, Japan, [7]Human Genome Center, Institute of Medical Science, University of Tokyo, Tokyo, Japan and [8]Department of Neurology, Kawasaki Medical School, Kurashiki, Japan

Received December 5, 2002; Revised March 21, 2003; Accepted April 10, 2003 DDBJ/EMBL/GenBank accession no. AB077383

Fukuyama-type congenital muscular dystrophy (FCMD), one of the most common autosomal-recessive disorders in Japan, is characterized by congenital muscular dystrophy associated with brain malformation due to a defect during neuronal migration. Through positional cloning, we previously identified the gene for FCMD, which encodes the fukutin protein. Here we report that chimeric mice generated using embryonic stem cells targeted for both *fukutin* alleles develop severe muscular dystrophy, with the selective deficiency of α-dystroglycan and its laminin-binding activity. In addition, these mice showed laminar disorganization of the cortical structures in the brain with impaired laminin assembly, focal interhemispheric fusion, and hippocampal and cerebellar dysgenesis. Further, chimeric mice showed anomaly of the lens, loss of laminar structure in the retina, and retinal detachment. These results indicate that fukutin is necessary for the maintenance of muscle integrity, cortical histiogenesis, and normal ocular development and suggest the functional linkage between fukutin and α-dystroglycan.

INTRODUCTION

Since the discovery of the Duchenne muscular dystrophy (DMD) gene product dystrophin (1), many studies have focused on understanding the pathophysiology of muscular dystrophies and on developing therapeutic approaches. Structural defects in the dystrophin–glycoprotein complex (DGC) can result in a loss of linkage between laminin-2 (merosin) in the extracellular matrix and actin in the subsarcolemmal cytoskeleton, and this can lead to various muscular dystrophies (2). Of these, α-dystroglycan is a heavily glycosylated mucin-type glycoprotein on the surface of muscle cells (3–5). It is the key component of the DGC, providing a tight linkage between the cell and basement membranes by binding laminin via its carbohydrate residues (3–5). α-Dystroglycan plays an active role in the basement membrane assembly itself (6).

Fukuyama-type congenital muscular dystrophy (FCMD), one of the most common autosomal-recessive disorders in Japan, is characterized by congenital muscular dystrophy associated with brain malformation (polymicrogyria) due to a defect during neuronal migration (7). Patients with FCMD manifest

*To whom correspondence should be addressed. Tel: +81 668793380; Fax: +81 668793389; Email: toda@clgene.med.osaka-u.ac.jp

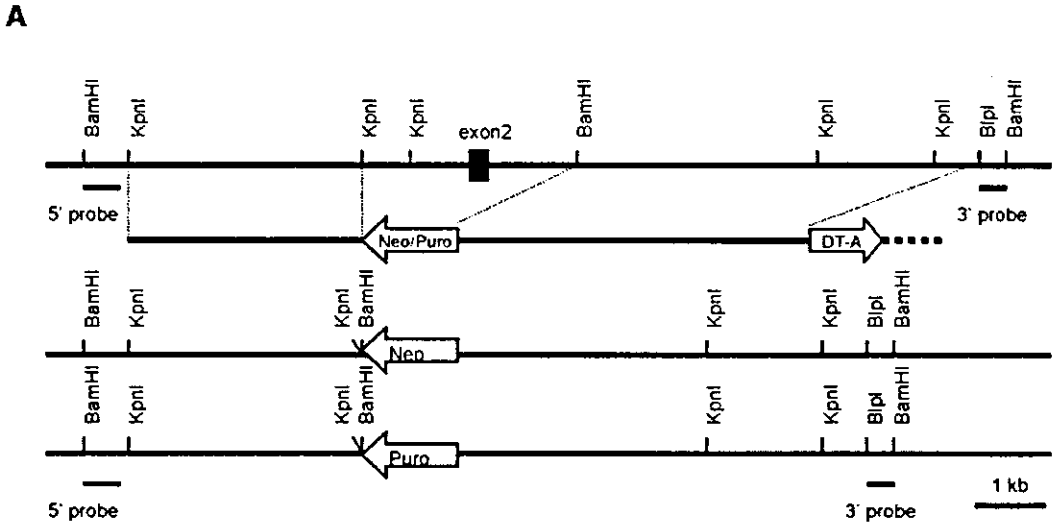
A
BamHI
KpnI
exon2
BlpI
5' probe
3' probe
Neo/Puro
DT-A
Neo
Puro
1 kb

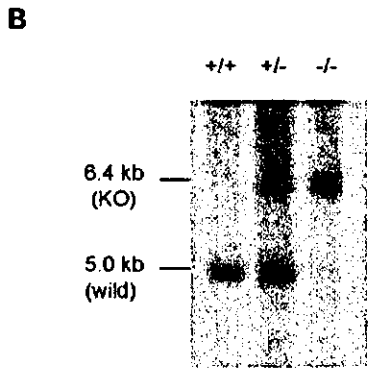
B
+/+
+/-
-/-
6.4 kb
(KO)
5.0 kb
(wild)

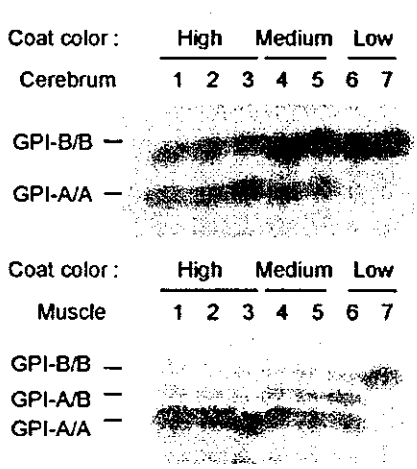
C
Coat color :
High
Medium
Low
Cerebrum
1 2 3 4 5 6 7
GPI-B/B
GPI-A/A
Muscle
GPI-A/B

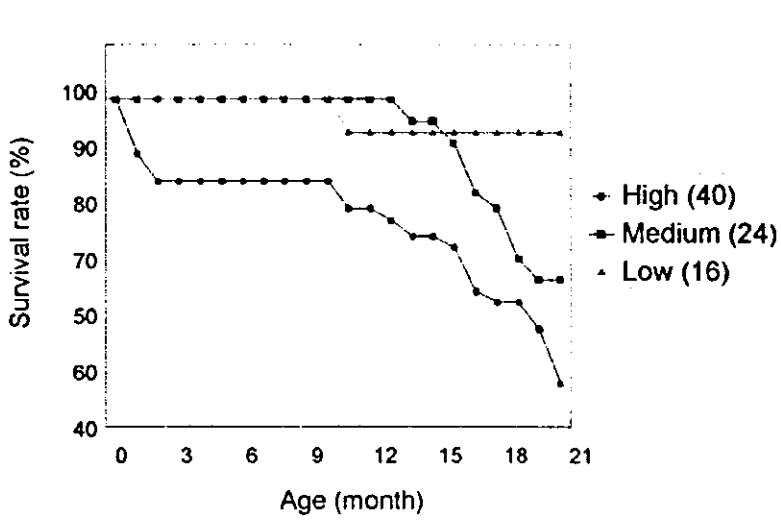
D
Survival rate (%)
100
90
80
70
60
50
40
0 3 6 9 12 15 18 21
Age (month)
High (40)
Medium (24)
Low (16)

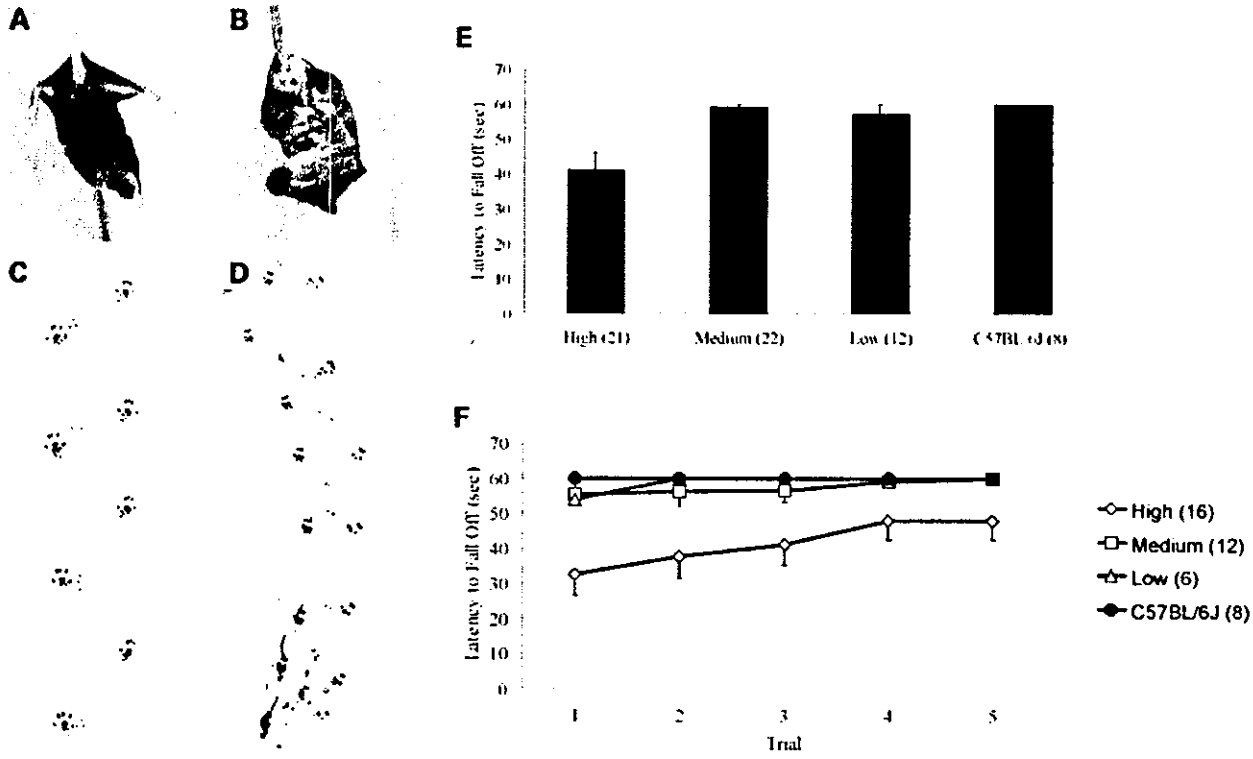

Figure 2. Behavioral abnormalities of fukutin-deficient chimeric mice. (**A** and **B**) When lifted by the tail, wild-type (C57BL/6J) mice extended their limbs (A), whereas chimeric mice folded their limbs towards the trunk (B). (**C** and **D**) Walking footprints. In contrast with wild-type mice (C), chimeric mice could not walk along a straight line and dragged their feet (D). (**E** and **F**) Hanging wire grip test (E) and Rotor-rod test (F). In both tests, the chimeric mice with coat colors indicating a high contribution of fukutin-deficient cells (high) fell with a shorter latency than either wild-type mice or chimeric mice with a lower contribution of fukutin-deficient cells (medium and low). The number of mice examined is shown in parentheses. $^{*}P < 0.05$.

weakness of facial and limb muscles, and general hypotonia which usually appears before 9 months of age. Functional disability is more severe in FCMD patients than in DMD patients; usually the maximum level of motor function achieved is sliding while sitting on the buttocks, and most FCMD patients are never able to walk. Patients usually become bedridden before 10 years of age due to generalized muscle atrophy and joint contracture, and most of them die by 20 years of age. Another manifestation observed in all cases is severe mental retardation; IQ scores in most FCMD patients lie between 30 and 50. Seizures occur in nearly half of the cases, in association with abnormal electroencephalograms (7).

Through positional cloning, we previously identified the gene responsible for FCMD, which encodes the fukutin protein (8–10). Most FCMD patients carry an ancestral mutation (11), which arose as a consequence of the integration of a 3 kb retrotransposon element into the 3′ untranslated region of the *fukutin* gene (10). FCMD is the first known human disease to be caused by an ancient retrotransposal integration. No FCMD patients have been identified with non-founder (point) mutations on both alleles, suggesting that such patients are embryonic-lethal and that fukutin is essential for normal development (12). There are no reported naturally occurring mice carrying mutations in the *fukutin* gene. Targeted homozygous mutation of this gene in mice leads to lethality at embryonic day 6.5–7.5, prior to development of skeletal muscle, cardiac muscle or mature neurons, suggesting that fukutin is essential for early embryonic development

Figure 1. Targeted disruption of both copies of *fukutin* in ES cells. (**A**) Physical map of the *fukutin* wild-type locus containing exon 2, targeting vector harboring the neomycin (neo^r) or puromycin (puro^r) resistant gene, and the disrupted *fukutin* locus. The arrowhead indicates the orientation of the drug-resistance genes. (**B**) Southern blot of *BamH*I-digested ES cell genomic DNA with the 3′ probe depicted in (A). A 5.0 kb wild-type fragment is detected in the single copy neo^r targeted clone (lane 2) as in parental ES cells (lane 1). In the double-copy targeted clone (lane 3), only a 6.4 kb band corresponding to the mutant allele was detected. (**C**) Contribution of *fukutin*-disrupted ES cells to brain and skeletal muscle. 129/SvEv and C57BL/6J mouse strains from which the *fukutin*-disrupted and wild-type tissues were derived have distinct electrophoretic variants of the two subunits of the glucose phosphate isomerase (129/SvEv, Gpi-1a; C57BL/6J, Gpi-1b). In correspondence with the coat color of the chimeric mice, the contribution of *fukutin*-deficient cells was high (lanes 1–3), medium (lanes 4 and 5), and low (lanes 6 and 7). (**D**) Survival rate of chimeric mice. The number of mice examined is shown in parentheses.

(Kurahashi *et al.*, unpublished data). To test the hypothesis that fukutin is necessary for maintenance of muscle integrity or histiogenesis of cerebral and cerebellar cortices, we here generated fukutin-deficient chimeric mice using embryonic stem (ES) cells targeted for both *fukutin* alleles. Interestingly, they also showed anomaly of the lens, loss of laminar structure in the retina, and retinal detachment. Our results indicate that fukutin is necessary for the maintenance of muscle integrity, cortical histiogenesis and normal ocular development, and suggest functional linkage between fukutin and α-dystroglycan.

RESULTS

Generation of fukutin-deficient chimeric mice

We used targeting vectors to generate ES cells in which both *fukutin* alleles have been disrupted by homologous recombination. To design a targeting vector for the generation of fukutin-deficient chimeric mice, we characterized a cosmid clone spanning exons 1–5 of the mouse *fukutin* gene (13) isolated from a 129/SvEv mouse library. The 2.3 kb *KpnI–BamHI* fragment containing the first coding exon (exon 2) was replaced with either a neomycin or a puromycin resistance gene (Fig. 1A), thereby removing the coding sequence corresponding to amino acids 1–35, as well as the splicing donor and acceptor sites. Targeted *fukutin* gene disruption was confirmed by Southern blot analysis of genomic DNA from ES cells (Fig. 1B).

After seven rounds of blastocyst injections, a total of 62 mice were born that were determined to be highly chimeric because of their coat color (agouti). Glucose phosphate isomerase isozyme (Gpi) assay revealed that the extent of chimerism in various tissues corresponded well with that determined by coat color (Fig. 1C). Therefore, we classified chimeric mice into three groups depending on chimerism of coat color (high, over 70% contribution of fukutin$^{-/-}$ cells; medium, 70–20%; and low, under 20%). Body weight was lower in the agouti mice (highly chimeric), and some died within one month. From 12 months of age, survival rates of high and medium chimeras gradually decreased. At 21 months survival rates of high, medium and low chimeras were 48, 67 and 94%, respectively (Fig. 1D).

Behavioral abnormalities in fukutin-deficient chimeric mice

Chimeric mice were dystrophic, although those with 50% or greater contribution from heterozygous ES cells showed no obvious phenotype, consistent with the lack of phenotype in fukutin$^{+/-}$ mice (Kurahashi *et al.*, unpublished data). Agouti mice (high) developed clasping when suspended by the tail (Fig. 2A and B). Analysis of hind footprints showed that they were unable to walk in a straight line and dragged their feet (Fig. 2C and D). Chimeras also showed muscle weakness in the hanging wire grip test (Fig. 2E) and positional instability in the rotor-rod test (Fig. 2F). These features first appeared at about 1 month but were not progressive.

Muscular dystrophic changes in fukutin-deficient chimeric mice

Figure 3A shows the histology of skeletal muscle in the hindlimbs of fukutin-deficient chimeric mice (high, lanes 1–3 in Fig. 1C). Massive necrosis with phagocytosis, mononuclear cell infiltration, basophilic regenerating muscle fibers, and increase of interstitial connective tissue were present at 1 month after birth. At later stages (7–9 months), a large number of small-sized muscle fibers contained central nuclei, indicating active regeneration. A small number of muscle fibers were undergoing degeneration and phagocytosis by macrophages. Connective tissue hyperplasia and fat cell deposition were also present.

α-Dystroglycan, a component of the DGC, is a heavily glycosylated mucin-type glycoprotein on the surface of muscle cells (3–5). It is the key component of the DGC, providing a tight linkage between the cell and basement membranes by binding laminin via its carbohydrate residues (3–5). α-Dystroglycan plays an active role in the basement membrane assembly itself (6). It was demonstrated recently that α-dystroglycan was selectively deficient in skeletal muscle from FCMD patients (14). We thus investigated the expression of α-dystroglycan, as well as the other components of the DGC, in skeletal muscle from fukutin-deficient chimeric mice by immunohistochemistry. α-Dystroglycan was greatly reduced in the sarcolemma of most muscle fibers in chimeric mice, while the other proteins, including β-dystroglycan and laminin α2 chain, were preserved (Fig. 3B). Interestingly, all regenerating muscle fibers were deficient in α-dystroglycan, suggesting that the fukutin deficiency did not significantly interfere with muscle fiber regeneration. Anti-fukutin antibody reacts with Golgi only in normal cell lines transfected with fukutin, not in non-transfected normal cells or normal human muscle, suggesting that the expression level of endogenous fukutin may be low (Kobayashi *et al.*, unpublished data). As muscle fibers are multi-nucleated, *in situ* hybridization for the targeting vector neo^r did not show complete correspondence between neo^r-positive and α-dystroglycan-negative fibers, although most neo^r-positive fibers were α-dystroglycan-negative (data not shown).

Immunoblot analysis confirmed the reduction of α-dystroglycan, especially in the antibody against the laminin-binding sugar chain of α-dystroglycan (IIH6; Fig. 3C). In addition, laminin blot overlay analysis revealed a deficiency in the laminin-binding activity of α-dystroglycan in chimeric mice (Fig. 3C). These results indicate that the linkage between laminin-2 and α-dystroglycan on the sarcolemma is disrupted in chimeric mice.

Brain anomalies in fukutin-deficient chimeric mice

We found markedly disorganized laminar structures in the cerebral and cerebellar cortices and hippocampus of fukutin-deficient chimeric mice. In the cerebral cortex, the normal six-layered structure was not clearly discernible (Fig. 4A and B). In some areas, cortical neurons had overmigrated, and the molecular layer (layer I) of the cerebral cortex had disappeared. The midline interhemispheric fissure was partially deficient, with fusion of medial surfaces of the cerebral cortex (Fig. 4C

and D). A small number of pyramidal cells in the CA3 sector of the hippocampus were not laminated, although the majority of pyramidal cells were aggregated in a compact lamina. Granule cells in the dentate gyrus were aggregated in a distorted, wavy distribution (Fig. 4E and F). In the cerebellum, the development of folia was defective, and the cerebellar fissure between the adjoining folia were partially fused. The granular layer was disorganized along the fusion lines of adjacent folia or at the pia matter, and Purkinje cells were sporadically malpositioned. Fusions between the caudal surface of the inferior colliculus and the rostral surface of the cerebellum were also observed (Fig. 4G and H).

After the injection of horseradish peroxidase (HRP) into the lumbar cord, corticospinal neurons with pyramidal somata were retrogradely labeled. While the somata of HRP-labeled corticospinal neurons were situated exclusively in layer V in the motor-sensory cortex of control mice (Fig. 4I and K), they were not distributed in any specific zone but were scattered diffusely throughout all depths of the cortex in chimeric mice (Fig. 4J and L).

Immunostaining with anti-laminin antibody revealed irregular interruptions of the meningeal basement membrane and granular deposits of laminin in the disorganized cerebral cortex (Fig. 4M and N). The meningeal basement membrane was also deficient over the fused medial cortex along the midline interhemispheric fissure or the fused cerebellar folia along the cerebellar sulci (data not shown). In contrast, the basement membrane surrounding blood vessels in the brain parenchyma was preserved. These findings indicate that fukutin is required for the assembly and/or remodeling of the meningeal basement membrane during the developmental period of brain cortical structures.

Immunoblot analysis revealed that α-dystroglycan was greatly reduced in the cerebral surface in chimeric mice and laminin blot overlay analysis revealed a deficiency in the laminin-binding activity of α-dystroglycan in chimeric mice (Fig. 4O). These results were similar to those in skeletal muscle and suggest that abnormal laminin–dystroglycan complex possibly cause brain anomalies in chimeric mice.

Eye anomalies in fukutin-deficient chimeric mice

Eye findings were quite remarkable. Fukutin-deficient chimeric mice showed corneal opacification with vascular infiltration (Fig. 5A and B). Microscopic analysis revealed a number of anomalies, including anomalous formation of the eyeball and lens (Fig. 5C and D); loss of laminar structure of the retina and retinal detachment (Fig. 5E and F); extensive folding of the retina (Fig. 5G); and thickened cornea with granular tissue formation, adhesion of the lens and cornea, and corneal inflammation and degeneration (Fig. 5H). Electroretinography (ERG) revealed extinction of the b-wave (Fig. 5I).

DISCUSSION

Here we have generated chimeric mice deficient in fukutin and shown that, similar to FCMD patients, the mutant mice develop neuronal migration disorder and ocular abnormality in addition to severe muscular dystrophy. At present, the function of fukutin remains unknown, and the mechanism by which its

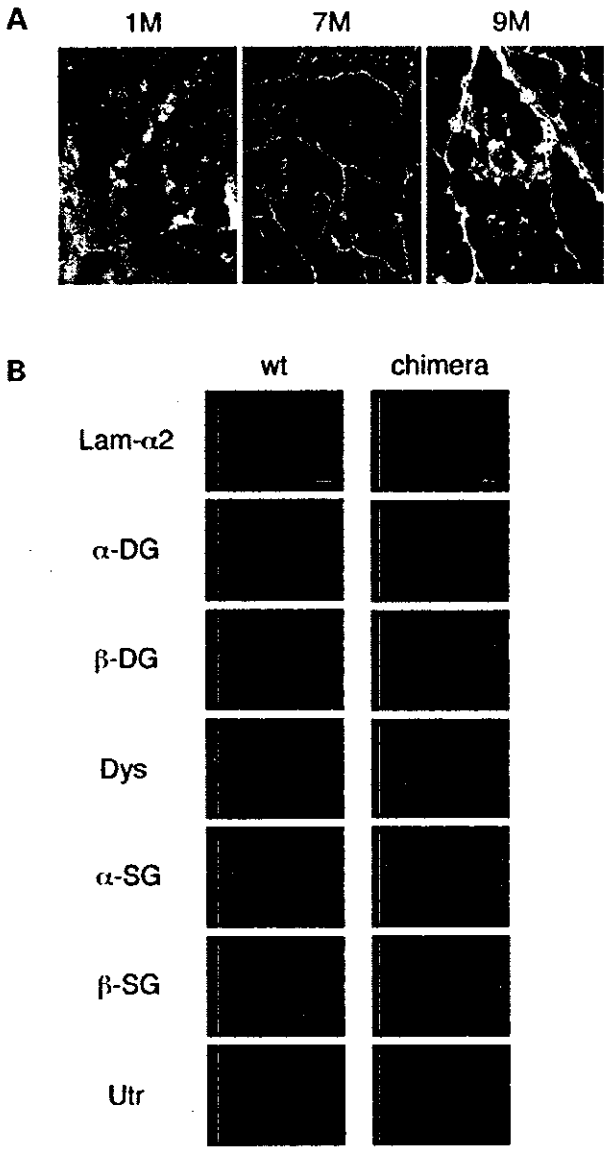

Figure 3. Muscular dystrophic changes in fukutin-deficient chimeric mice. (**A**) HE stained quadriceps muscle of chimeric mice. Massive necrosis with phagocytosis (asterisk), mononuclear cell infiltration (arrowhead), basophilic regenerating fibers (arrow), and an increase in connective tissue mass was present at 1 month of age. At the late stages of 7–9 months, a large number of small-sized fibers were found to have central nuclei (arrowhead), while a small number of fibers were undergoing active degeneration (arrow). Scale bar, 100 μm. (**B**) Immunohistochemical analysis of sarcolemmal proteins in quadriceps muscle from normal (wt) and chimeric mice. Lam-α2, laminin α2 chain; DG, dystroglycan; Dys, dystrophin; SG, sarcoglycan; Utr, utrophin. Selective and scattered deficiency of α-dystroglycan was observed in chimeric mice, while the other proteins were preserved. Scale bar, 100 μm. (C) Immunoblot and laminin blot overlay analyses of quadriceps muscle from the two normal (wt) and three chimeric mice. α-Dystroglycan immunoreactivity, as well as its laminin-binding activity, was greatly reduced in chimeric mice, while β-dystroglycan and laminin α2 chain were preserved. The deficiency of α-dystroglycan revealed by laminin blot overlay paralleled that revealed by monoclonal antibody IIH6C4 and was more prominent than that revealed by monoclonal antibody VIA4-1

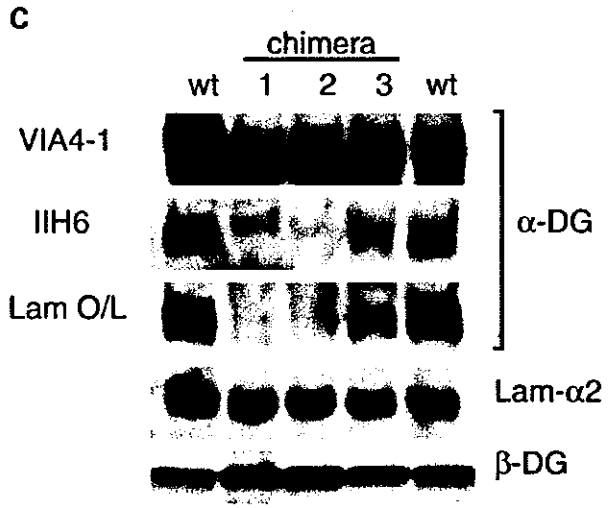

Figure 3 *continued.*

deficiency causes defects in multiple organs has not been clarified. In this respect, it should be noted that sequence analysis predicts fukutin to be an enzyme that modifies cell-surface glycoproteins or glycolipids (15). There are several lines of indirect but significant evidence to support this. First, it was reported that highly glycosylated α-dystroglycan was selectively deficient in the skeletal muscle of FCMD patients (14). Second, we have reported that muscle–eye–brain disease (MEB), an autosomal-recessive disorder having skeletal muscle, eye and brain defects similar to FCMD (16), is caused by mutations in the gene encoding the protein *O*-linked mannose β1, 2-*N*-acetylglucosaminyltransferase (POMGnT1), which cause the loss of the enzyme activity (17). Moreover, we have found the selective deficiency of α-dystroglycan in the skeletal muscle of MEB patients (18). Finally, defective glycosylation of α-dystroglycan has also been reported in another form of congenital muscular dystrophy, MDC1C, caused by mutations in the gene encoding the putative glycosyltransferase named FKRP (fukutin-related protein) (19) and in *myd* mice, an animal model of congenital muscular dystrophy, caused by the mutation in the gene encoding a putative glycosyltransferase named Large (20), although brain and eye anomalies are not the hallmarks of MDC1C. Quite recently 20% of Walker–Warburg syndrome patients have been found to have mutations in POMT1, a putative human counterpart of yeast O-mannosyltransferase (21). Moreover, Michele *et al.* (22) showed, in MEB, FCMD and myodystrophy mouse, that α-dystroglycan is expressed at the muscle membrane, but similar hypoglycosylation in the diseases directly abolishes binding activity of dystroglycan for the ligands laminin, neurexin and agrin. Together with the present results, these findings suggest that defective glycosylation of α-dystroglycan due to the primary genetic defects of glycosyltransferases may be the common denominator causing muscle cell degeneration in these diseases.

Strikingly, the deficiency of α-dystroglycan revealed by laminin blot overlay paralleled that revealed by the monoclonal antibody IIH6C4, which recognizes the laminin-binding carbohydrate residues of α-dystroglycan, and was more prominent than that revealed by the monoclonal antibody VIA4-1, which recognizes carbohydrate residues unrelated to the binding of laminin (4,23) (Figs 3C and 4O). It is of course possible that α-dystroglycan is still present but in a hypoglycosylated form, as was suggested to occur in FCMD by Michele *et al.* (22). This raises the possibility that fukutin may be involved in the modification of laminin-binding carbohydrate residues in α-dystroglycan and, in the absence of fukutin, the linkage between laminin and α-dystroglycan may never be established on the muscle cell surface. This scenario is also consistent with the report that chimeric mice lacking skeletal muscle dystroglycan developed muscular dystrophy similar to the mice described here (24).

Finally, the role of dystroglycan in the pathogenesis of brain and eye defects in FCMD remains unclear. Brain and/or eye defects similar to those reported here have recently been observed in mice lacking dystroglycan in the brain via Cre/*loxP*-mediated gene inactivation (25) and in *myd* mice, although the retina was apparently morphologically normal (26). Interestingly, brain and/or eye defects similar to those reported here have also been observed in mice lacking integrin β1 subunit in brain via Cre/*loxP*-mediated gene inactivation (27) and in mice carrying a targeted mutation in the integrin α6 subunit gene (28), respectively. We can envisage that the defects in dystroglycan have similar consequences as those caused by integrin deficiency, because these two receptors are thought to work in concert. Alternatively, fukutin might be involved in the modification of the carbohydrate residues of integrin subunits in brain and eye, and integrin might not function normally in the absence of fukutin, although immunostaining for integrin α7 on skeletal muscle cryosections showed no difference (data not shown).

Our data indicates that fukutin is essential for maintenance of muscle integrity, cortical histiogenesis, and normal eye development and suggest the functional linkage between fukutin and α-dystroglycan. Fukutin-deficient chimeric mice are suitable models for studying not only the biological function of fukutin but also the molecular pathogenesis of and therapeutic approaches to complex disorders exhibiting the simultaneous occurrence of central nervous, ocular and muscular abnormalities seen in FCMD and its related diseases.

MATERIALS AND METHODS

Targeted disruption of *fukutin*

A cosmid clone spanning exons 1–5 of the mouse *fukutin* gene was isolated from a 129/SvEv mouse library. Two targeting vectors were constructed with a 12 kb *Kpn*I–*Blp*I fragment containing the first coding exon (exon 2) and flanking introns. The 2.3 kb *Kpn*I–*Bam*HI fragment containing exon 2 was replaced with either a neomycin or a puromycin resistance gene (pKO-Select Neo or pKO-Select Puro, Lexicon), thereby removing the coding sequence corresponding to amino acids 1–35, as well as the splicing donor and acceptor sites. Targeting vectors were linearized using *Not*I, and AB2.2 prime ES cells (Lexicon) were first electroporated with the neo^r vector. We

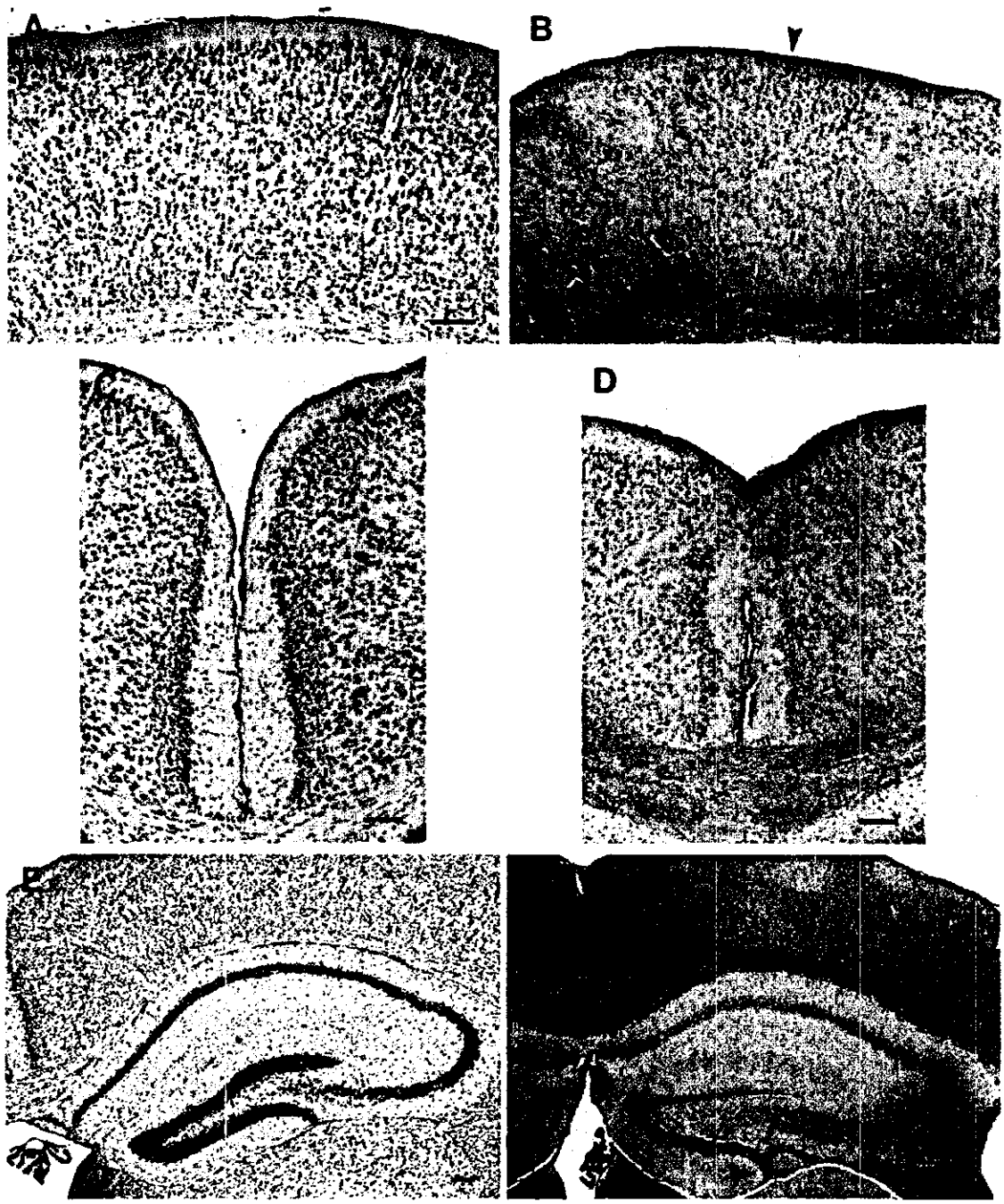

Figure 4. Brain anomalies in fukutin-deficient chimeric mice. (**A–H**) HE-stained sections of brain from normal (A, C, E and G) and chimeric (B, D, F and H) mice. (A and B) cerebral cortex; (C and D) interhemispheric fissure; (E and F) hippocampus and dentate gyms; (G and H) cerebellum. In chimeric mice, cerebral cortical neurons overmigrated, and the molecular layer was absent (arrowhead) (B). The midline interhemispheric fissure was absent due to the fusion of the adjoining medial surfaces of the cerebral cortex (arrowhead) (D). A single laminar distribution of pyramidal neurons was disorganized in the CA3 sector of the hippocampus (asterisk), and dentate granular cells were aggregated in a distorted wavy distribution (arrowhead) (F). The granular cell layer in the cerebellar cortex was disorganized along the fused cerebellar folia (asterisk) (H). (**I–L**) HRP retrograde labeling of cerebral cortex from normal (I and K) and chimeric (J and L) mice. In chimeric mice, HRP-labeled corticospinal neurons were not localized in layer V but scattered throughout all the depths of the motor cortex. (**M** and **N**) Laminin immunostaining of cerebral surface from normal (M) and chimeric (N) mice. In chimeric mice, the basement membrane was interrupted (arrowhead), and laminin was deposited in sporadic granules (asterisk) in the cerebral cortex. Scale bar, 100 μm. (**O**) Immunoblot and laminin blot overlay analyses of cerebral surface from the three normal (wt) and four chimeric mice. α-dystroglycan immunoreactivity, as well as its laminin-binding activity, was greatly reduced in chimeric mice. The results were similar to those in skeletal muscle (Fig. 3C).

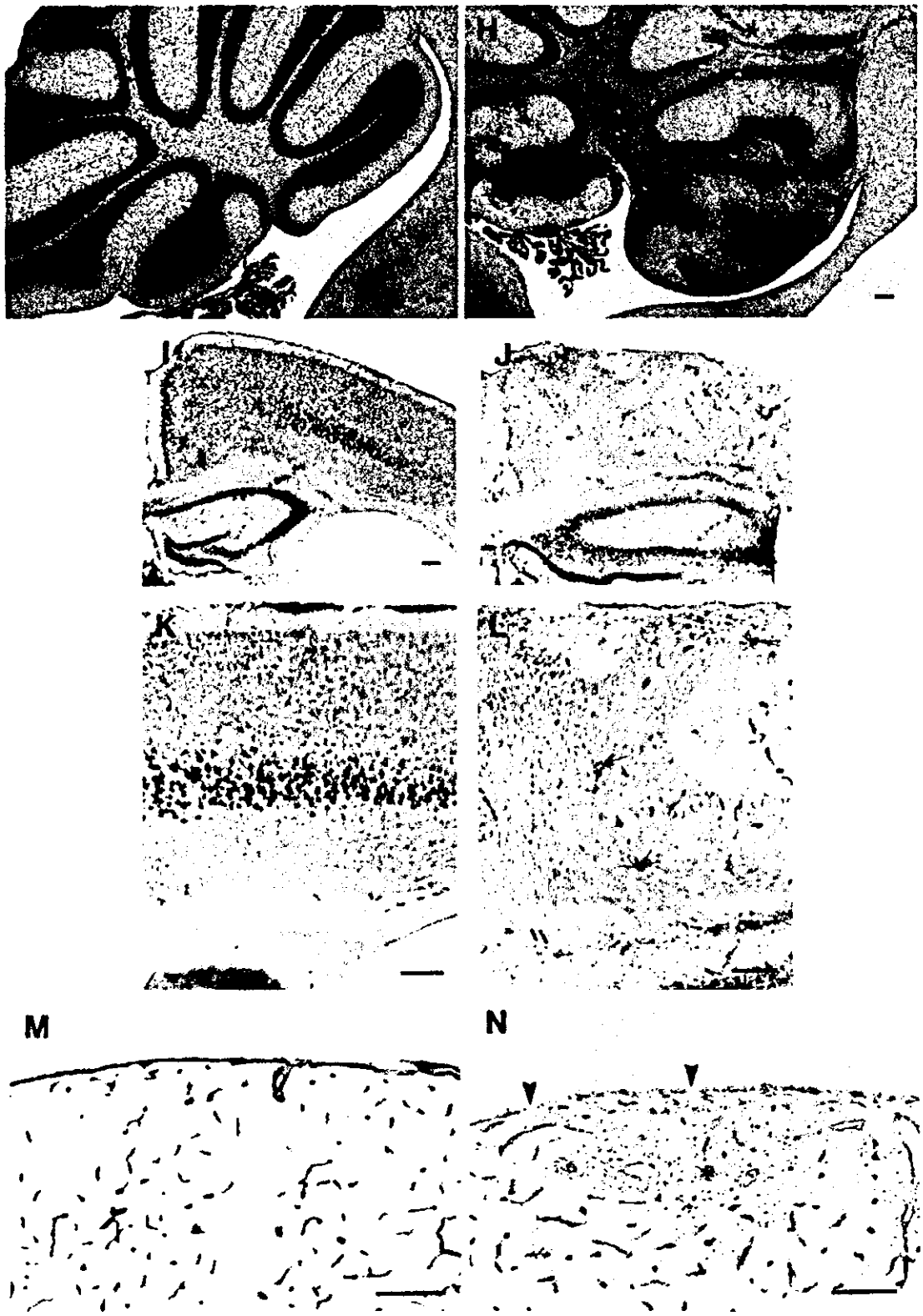

Figure 4 *continued.*

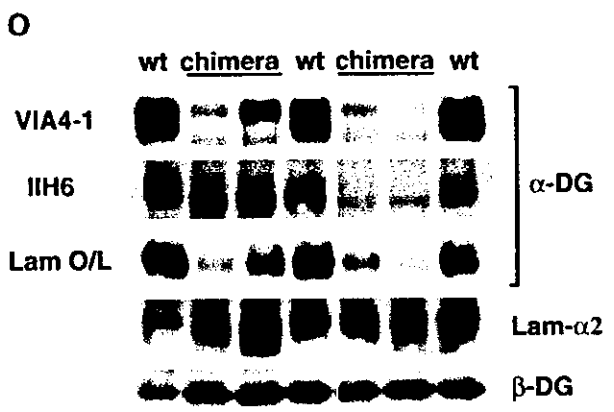

Figure 4 *continued.*

picked, expanded and screened Geneticin-resistant (Sigma) clones for homologous recombination. One clone (no. 8) was chosen and electroporated with the puro^r vector. Puromycin-resistant clones were screened to identify homologous recombinant clones. The double copy-targeted ES cell clone P182 was injected into E3.5 blastocysts of the C57BL/6 mouse strain using standard methods. Mice were maintained in accordance with the Animal Care guidelines of Otsuka Pharmaceutical Co. Ltd.

Evaluation of fukutin-null ES cell contribution to chimeric mice

Mice were sacrificed between 1 and 9 months of age. Protein extracts from tissue samples were subjected to Gpi electrophoresis, and the Gpi variants were stained on the cellulose acetate gels (Helena).

Behavioral phenotyping

Mice were tested during the light phase of their light-dark cycle between 13:00 and 17:00. Mice 7–9 months old were placed on the rotor-rod treadmill apparatus (rod diameter, 3 cm, MK-600, Muromachi Kikai) for a maximum of 60 s, and the latency to fall off the rod within the time period was recorded. Five consecutive trials were performed at 12 rpm. The hanging wire test was carried out by placing 5- to 7-month-old mice on top of the wire cage lid and turning the lid upside down. The latency to fall off the wire was measured up to 60 s. To record the footprint pattern, hindpaws were dipped in India ink, and mice were allowed to walk along a 35 cm long, 10 cm wide runway with 6 cm high walls. The footprints were recorded on a clean sheet of white paper placed on the floor of the dark tunnel. All mice were given one training run per week for 3 weeks before being subjected to a test run.

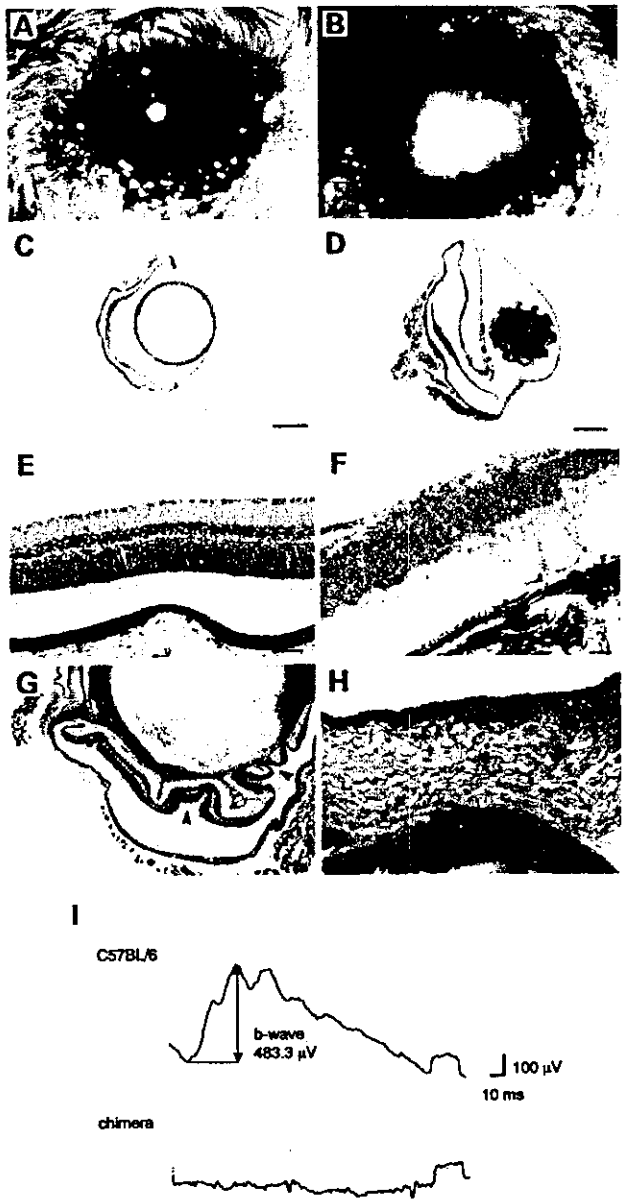

Figure 5. Eye anomalies in fukutin-deficient chimeric mice. (A and B) Gross appearance of eyes from normal (A) and chimeric (B) mice. In chimeric mice, corneal and/or lens opacification was present (B). (C–H) HE-stained sections of eyeballs from normal (C and E) and chimeric (D, F–H) mice. In chimeric mice, the lens had a peculiar shape, with the sclera bent and intercalated between the lens and retina (D). The laminar structure of the retina was completely disorganized and retinal detachment was present (F). The retina was misfolded extensively in a wavy pattern (arrowhead) (G). The cornea was thickened by granular tissue formation (asterisk) and adhered to the lens with inflammation (arrowhead) (H). Scale bar, C and D, 1.3 mm; E–H, 100 μm. (I) ERG revealed extinction of the b-wave.

Histology and immunohistochemistry

Animals were anesthetized with ether and exsanguinated. Brains and eyes were removed and fixed with 10% formalin in 10 mM phosphate buffer (pH 7.2) for 4 days. After paraffin embedding, cerebrums were sectioned serially to 8 μm thickness at coronale. Cerebellums and eyeballs were sectioned to

8 μm thickness at sagittal. Every tenth section was counter-stained with hematoxylin and eosin (HE) or by Klüver–Barrera's (KB) methods. Several adjoining sections were immunostained with a polyclonal anti-laminin antibody (Harber Bio-products). For skeletal muscle, serial frozen cryosections (8 μm) were stained with HE or immunostained with the monoclonal α-dystroglycan antibody VIA4-1 (Upstate) or antisera against laminin α2 chain (29), β-dystroglycan (30), dystrophin (31), α-sarcoglycan (29), β-sarcoglycan (32), and utrophin (30). After incubation with Alexa Fluor 488-labeled secondary antibodies (Molecular Probes), sections were examined under a fluorescent microscope.

Immunoblot and laminin blot overlay

SDS–PAGE, 3–12%, and immunoblotting of skeletal muscle and cerebral surface cryosections were performed as described previously (33), using the monoclonal antibodies IIH6C4 and VIA4-1 against α-dystroglycan (Upstate), the antiserum against β-dystroglycan, and the monoclonal antibody 2D9 against the laminin α2 chain (34). The laminin blot overlay was performed using 3 nM laminin-1 (Koken), and the laminin bound to α-dystroglycan on the polyvinylidene difluoride membrane was detected using a polyclonal anti-laminin antibody (Sigma).

HRP labeling

One microliter of 10% aqueous solution of HRP (type VI, Sigma) was injected into both sides of the upper lumbar cord. After 48 h, the animals were transcardially perfused with 1.25% glutaraldehyde and 1% paraformaldehyde in 0.1 M phosphate buffer (pH 7.4). The brain and spinal cord were immersed in 30% phosphate-buffered sucrose overnight at 4°C, sectioned coronally at 40 μm thickness on a freezing microtome, and reacted for the presence of HRP using the chromagen tetramethylbenzidine (TMB) (35).

Electroretinography

Following 15 min of dark adaptation, ERGs were recorded from the corneal surface electrode after mydriasis. Stimulation with white flash light (10 J) was used (Photostimulator 3G21, NEC-Sanei).

ACKNOWLEDGEMENTS

We thank Drs Masato Horie, Ei-ichi Takahashi, Kenji Araishi, Yukiko K. Hayashi and Eva Engvall for discussion and antibodies; Sawako Muroi, Takashi Wadatsu, Noritaka Koseki, Norihiro Miyazawa, Yuji Fujimori, Tomoyuki Iwanaga, Mai Okano and Kuniko Ohmori for assistance; and Dr Jennifer Logan for editing the manuscript. This study was supported by a Health Science Research Grant, 'Research on Brain Science' (H12-Brain-017) and by a Research Grants for Nervous and Mental Disorders (14B-4), both from the Ministry of Health, Labor and Welfare of Japan.

REFERENCES

1. Hoffman, E.P., Brown, R.H. Jr. and Kunkel, L.M. (1987) Dystrophin: the protein product of the Duchenne muscular dystrophy locus. *Cell*, **51**, 919–928.
2. Campbell, K.P. (1995) Three muscular dystrophies: loss of cytoskeleton–extracellular matrix linkage. *Cell*, **80**, 675–679.
3. Ibraghimov-Beskrovnaya, O., Ervasti, J.M., Leveille, C.J., Slaughter, C.A., Sernett, S.W. and Campbell, K.P. (1992) Primary structure of dystrophin-associated glycoproteins linking dystrophin to the extracellular matrix. *Nature*, **355**, 696–702.
4. Ervasti, J.M. and Campbell, K.P. (1993) A role for the dystrophin-glycoprotein complex as a transmembrane linker between laminin and actin. *J. Cell. Biol.*, **122**, 809–823.
5. Chiba, A., Matsumura, K., Yamada, H., Inazu, T., Shimizu, T., Kusunoki, S., Kanazawa, I., Kobata, A. and Endo, T. (1997) Structures of sialylated *O*-linked oligosaccharides of bovine peripheral nerve α-dystroglycan. The role of a novel *O*-mannosyl-type oligosaccharide in the binding of α-dystroglycan with laminin. *J. Biol. Chem.*, **272**, 2156–2162.
6. Henry, M.D. and Campbell, K.P. (1998) A role for dystroglycan in basement membrane assembly. *Cell*, **95**, 859–870.
7. Fukuyama, Y., Osawa, M. and Suzuki, H. (1981) Congenital progressive muscular dystrophy of the Fukuyama types—clinical, genetic and pathological considerations. *Brain Dev.*, **3**, 1–29.
8. Toda, T., Segawa, M., Nomura, Y., Nonaka, I., Masuda, K., Ishihara, T., Sakai, M., Tomita, I., Origuchi, Y., Suzuki, M. *et al.* (1993) Localization of a gene for Fukuyama type congenital muscular dystrophy to chromosome 9q31-33. *Nat. Genet.*, **5**, 283–286.
9. Toda, T., Miyake, M., Kobayashi, K., Mizuno, K., Saito, K., Osawa, M., Nakamura, Y., Kanazawa, I., Nakagome, Y., Tokunaga, K. and Nakahori, Y. (1996) Linkage-disequilibrium mapping narrows the Fukuyama-type congenital muscular dystrophy (FCMD) candidate region to <100 kb. *Am. J. Hum. Genet.*, **59**, 1313–1320.
10. Kobayashi, K., Nakahori, Y., Miyake, M., Matsumura, K., Kondo-Iida, E., Nomura, Y., Segawa, M., Yoshioka, M., Saito, K., Osawa, M. *et al.* (1998) An ancient retrotransposal insertion causes Fukuyama-type congenital muscular dystrophy. *Nature*, **394**, 388–392.
11. Colombo, R., Bignamini, A.A., Carobene, A., Sasaki, J., Tachikawa, M., Kobayashi, K. and Toda, T. (2000) Age and origin of the FCMD 3′-untranslated-region retrotransposal insertion mutation causing Fukuyama-type congenital muscular dystrophy in the Japanese population. *Hum. Genet.*, **107**, 559–567.
12. Kondo-Iida, E., Kobayashi, K., Watanabe, M., Sasaki, J., Kumagai, T., Koide, H., Saito, K., Osawa, M., Nakamura, Y. and Toda, T. (1999) Novel mutations and genotype-phenotype relationships in 107 families with Fukuyama-type congenital muscular dystrophy (FCMD). *Hum. Mol. Genet.*, **8**, 2303–2309.
13. Horie, M., Kobayashi, K., Takeda, S., Nakamura, Y., Lyons, G.E. and Toda, T. (2002) Isolation and characterization of the mouse ortholog of the Fukuyama-type congenital muscular dystrophy gene. *Genomics*, **80**, 482–486.
14. Hayashi, Y.K., Ogawa, M., Tagawa, K., Noguchi, S., Ishihara, T., Nonaka, I. and Arahata, K. (2001) Selective deficiency of α-dystroglycan in Fukuyama-type congenital muscular dystrophy. *Neurology*, **57**, 115–121.
15. Aravind, L. and Koonin, E.V. (1999) The fukutin protein family—predicted enzymes modifying cell-surface molecules. *Curr. Biol.*, **9**, R836–837.
16. Santavuori, P., Somer, H., Sainio, K., Rapola, J., Kruus, S., Nikitin, T., Ketonen, L. and Leisti, J. (1989) Muscle–eye–brain disease (MEB). *Brain Dev.*, **11**, 147–153.
17. Yoshida, A., Kobayashi, K., Manya, H., Taniguchi, K., Kano, H., Mizuno, M., Inazu, T., Mitsuhashi, H., Takahashi, S., Takeuchi, M. *et al.* (2001) Muscular dystrophy and neuronal migration disorder caused by mutations in a glycosyltransferase, POMGnT1. *Dev. Cell*, **1**, 717–724.
18. Kano, H., Kobayashi, K., Herrmann, R., Tachikawa, M., Manya, H., Nishino, I., Nonaka, I., Straub, V., Talim, B., Voit, T. *et al.* (2002) Deficiency of α-dystroglycan in muscle-eye-brain disease. *Biochem. Biophys. Res. Commun.*, **291**, 1283–1286.
19. Brockington, M., Blake, D.J., Prandini, P., Brown, S.C., Torelli, S., Benson, M.A., Ponting, C.P., Estournet, B., Romero, N.B., Mercuri, E. *et al.* (2001) Mutations in the fukutin-related protein gene (FKRP) cause a form of congenital muscular dystrophy with secondary laminin α2 deficiency and abnormal glycosylation of α-dystroglycan. *Am. J. Hum. Genet.*, **69**, 1198–1209.

20. Grewal, P.K., Holzfeind, P.J., Bittner, R.E. and Hewitt, J.E. (2001) Mutant glycosyltransferase and altered glycosylation of α-dystroglycan in the myodystrophy mouse. *Nat. Genet.*, **28**, 151–154.
21. Beltrán-Valero de Bernabé, D., Currier, S., Steinbrecher, A., Celli, J., van Beusekom, E., van der Zwaag, B., Kayserili, H., Merlini, L., Chitayat, D., Dobyns, W.B. *et al.* (2002) Mutations in the O-mannosyltransferase gene *POMT1* give rise to the severe neuronal migration disorder Walker–Warburg syndrome. *Am. J. Hum. Genet.*, **71**, 1033–1043.
22. Michele, D., Barresi, R., Kanagawa, M., Saito, F., Cohn, R.D., Satz, J.S., Dollar, J., Nishino, I., Kelley, R.I., Somer, H. *et al.* (2002) Post-translational disruption of dytroglycan–ligand interactions in congenital muscular dystrophies. *Nature*, **418**, 417–422.
23. Matsumura, K., Chiba, A., Yamada, H., Fukuta-Ohi, H., Fujita, S., Endo, T., Kobata, A., Anderson, L.V., Kanazawa, I., Campbell, K.P. and Shimizu, T. (1997) A role of dystroglycan in schwannoma cell adhesion to laminin. *J. Biol. Chem.*, **272**, 13904–13910.
24. Cote, P.D., Moukhles, H., Lindenbaum, M. and Carbonetto, S. (1999) Chimaeric mice deficient in dystroglycans develop muscular dystrophy and have disrupted myoneural synapses. *Nat. Genet.*, **23**, 338–342.
25. Moore, S.A., Saito, F., Chen, J., Michele, D.E., Henry, M.D., Messing, A., Cohn, R.D., Ross-Barta, S.E., Westra, S., Williamson, R.A. *et al.* (2002) Deletion of brain dystroglycan recapitulates aspects of congenital muscular dystrophy. *Nature*, **418**, 422–425.
26. Holzfeind, P.J., Grewal, P.K., Reitsamer, H.A., Kechvar, J., Lassmann, H., Hoeger, H., Hewitt, J.E. and Bittner, R.E. (2002) Skeletal, cardiac and tongue muscle pathology, defective retinal transmission, and neuronal migration defects in the Large^{myd} mouse defines a natural model for glycosylation-deficient muscle–eye–brain disorders. *Hum. Mol. Genet.*, **11**, 2673–2687.
27. Graus-Porta, D., Blaess, S., Senften, M., Littlewood-Evans, A., Damsky, C., Huang, Z., Orban, P., Klein, R., Schittny, J.C. and Muller, U. (2001) β1-class integrins regulate the development of laminae and folia in the cerebral and cerebellar cortex. *Neuron*, **31**, 367–379.
28. Georges-Labouesse, E., Mark, M., Messaddeq, N. and Gansmuller, A. (1998) Essential role of α6 integrins in cortical and retinal lamination. *Curr. Biol.*, **8**, 983–986.
29. Araishi, K., Sasaoka, T., Imamura, M., Noguchi, S., Hama, H., Wakabayashi, E., Yoshida, M., Hori, T. and Ozawa, E. (1999) Loss of the sarcoglycan complex and sarcospan leads to muscular dystrophy in β-sarcoglycan-deficient mice. *Hum. Mol. Genet.*, **8**, 1589–1598.
30. Imamura, M., Araishi, K., Noguchi, S. and Ozawa, E. (2000) A sarcoglycan–dystroglycan complex anchors Dp116 and utrophin in the peripheral nervous system. *Hum. Mol. Genet.*, **9**, 3091–3100.
31. Hagiwara, Y., Sasaoka, T., Araishi, K., Imamura, M., Yorifuji, H., Nonaka, I., Ozawa, E. and Kikuchi, T. (2000) Caveolin-3 deficiency causes muscle degeneration in mice. *Hum. Mol. Genet.*, **9**, 3047–3054.
32. Noguchi, S., Wakabayashi, E., Imamura, M., Yoshida, M. and Ozawa, E. (2000) Formation of sarcoglycan complex with differentiation in cultured myocytes. *Eur. J. Biochem.*, **267**, 640–648.
33. Matsumura, K., Tome, F.M., Collin, H., Azibi, K., Chaouch, M., Kaplan, J.C., Fardeau, M. and Campbell, K.P. (1992) Deficiency of the 50K dystrophin-associated glycoprotein in severe childhood autosomal recessive muscular dystrophy. *Nature*, **359**, 320–322.
34. Hori, H., Kanamori, T., Mizuta, T., Yamaguchi, N., Liu, Y. and Nagai, Y. (1994) Human laminin M chain: epitope analysis of its monoclonal antibodies by immunoscreening of cDNA clones and tissue expression. *J. Biochem.*, **116**, 1212–1219.
35. Mesulam, M.M. (1978) Tetramethyl benzidine for horseradish peroxidase neurohistochemistry: a non-carcinogenic blue reaction product with superior sensitivity for visualizing neural afferents and efferents. *J. Histochem. Cytochem.*, **26**, 106–117.

ELSEVIER

Clinical Biochemistry 36 (2003) 339–344

CLINICAL BIOCHEMISTRY

Enzymatic diagnostic test for Muscle-Eye-Brain type congenital muscular dystrophy using commercially available reagents

Wenli Zhang[a], Jiri Vajsar[b,c], Pinjiang Cao[a], Galen Breningstall[d], Charlotta Diesen[e], William Dobyns[f], Ralph Herrmann[g], Anna-Elina Lehesjoki[e], Alice Steinbrecher[g], Beril Talim[h], Tatsushi Toda[i], Haluk Topaloglu[j], Thomas Voit[g], Harry Schachter[a,c,*]

[a]*Department of Structural Biology and Biochemistry, The Hospital for Sick Children, 555 University Avenue, Toronto, Ont. M5G 1X8, Canada*
[b]*Division of Neurology, The Hospital for Sick Children, 555 University Avenue, Toronto, Ont. M5G 1X8, Canada*
[c]*University of Toronto, 1 King's College Circle, Toronto, Ont. M5S 1A8 Canada*
[d]*Department of Neurology, University of Minnesota, 420 Delaware Street SE, Minneapolis, MN 55455, and the Noran Neurological Clinic, 910 East 26th Street, Minneapolis, Minnesota 55404*
[e]*Folkhälsan Institute of Genetics and Department of Medical Genetics, University of Helsinki, FIN-00014 Helsinki, Finland*
[f]*The University of Chicago, Departments of Human Genetics, Neurology and Pediatrics, 920 E. 58th Street, Chicago, IL 60637*
[g]*Department of Pediatrics and Pediatric Neurology, University of Essen, D-45122 Essen, Germany*
[h]*Department of Pediatric Pathology, Hacettepe Children's Hospital, Ankara 06100, Turkey*
[i]*Division of Functional Genomics, Department of Post-Genomics and Diseases, Osaka University Graduate School of Medicine, 2-2-B9 Yamadaoka, Suita, Osaka 565-0871, Japan*
[j]*Department of Pediatric Neurology, Hacettepe Children's Hospital, Ankara 06100, Turkey*

Objectives: Mutations disrupting the interaction of extra-cellular ligands and α-dystroglycan are responsible for an etiologically heterogeneous group of autosomal recessive congenital muscular dystrophies (CMD) that can have associated brain and eye abnormalities. The objective is to develop a diagnostic test for one of these CMDs, Muscle-Eye-Brain disease (MEB), due to mutations in the gene encoding Protein *O*-Mannosyl β-1,2-*N*-acetylglucosaminyltransferase 1 (POMGnT1).
Design and Methods: POMGnT1 enzyme activity was determined in extracts of muscle biopsies from four MEB patients and various controls using commercially available reagents.
Results: All four MEB muscle samples showed a highly significant decrease in POMGnT1 activity relative to controls.
Conclusions: The assay of POMGnT1 activity in MEB muscle provides a rapid and relatively simple diagnostic test for this disease. CMDs associated with brain malformations such as MEB, WWS and FCMD are heterogenous in clinical presentation and on radiologic examination, suggesting that POMGnT1 assays of muscle biopsies should be used as a screening procedure for MEB in all CMD patients associated with brain malformations.

Keywords: Diagnosis; Neuromuscular; Dystrophy; Muscle; Eye; Brain; Glycosyltransferase; *N*-acetylglucosaminyltransferase; Enzyme Assay

1. Introduction

Dystroglycan (dystrophin-associated glycoprotein) is a central component of a multimeric protein assembly called the dystrophin glycoprotein complex (DGC), which is present in skeletal muscle and is comprised of dystrophin and several other proteins [1,2]. Defects in the DGC appear to play critical roles in several muscular dystrophies due to disruption of basement membrane organization [2,3]. Dystroglycan is expressed in many cell types and composed of α- and β-subunits encoded by a single mRNA [4]. The protein is synthesized as a precursor propeptide that is posttranslationally cleaved and differentially glycosylated to yield α- and β-dystroglycans. α-Dystroglycan is an extracellular protein which binds both β-dystroglycan, a transmembrane protein, and various extra-cellular ligands such as the laminin α2 chain of merosin [5–8]. Dystrophin binds both β-dystroglycan and the intra-cellular contractile protein F-actin. Dystroglycan therefore acts as a link between the extra-cellular matrix and intra-cellular actin.

Mutations that disrupt the interaction between dystrophin and actin lead to a severe Becker muscular dystrophy phe-

* Corresponding author. Tel.: +1-416-813-5915; fax: +1-416-813-5022.
E-mail address: harry@sickkids.ca (H. Schachter).

doi:10.1016/S0009-9120(03)00036-5

Nomenclature

CMD congenital muscular dystrophy
DGC dystrophin glycoprotein complex
FCMD Fukuyama congenital muscular dystrophy
MDC1C Congenital Muscular Dystrophy 1C
MEB Muscle-Eye-Brain disease
OMIM Online Mendelian Inheritance in Man (http://www.ncbi.nlm.nih.gov/)
POMGnT1 Protein *O*-Mannosyl β-1,2-*N*-acetylglucosaminyltransferase 1
POMT1 Protein *O*-Mannosyltransferase 1
WWS Walker-Warburg syndrome

notype whereas disruption of the β-dystroglycan-dystrophin interaction leads to a Duchenne muscular dystrophy phenotype [1,9]. Mutations disrupting the interaction of extracellular ligands and α-dystroglycan are responsible for an etiologically heterogeneous group of autosomal recessive congenital muscular dystrophies (CMD) that can have associated brain and eye abnormalities [10–14]. The diagnostic criteria for CMD include onset of muscle weakness at birth or first few months of life and dystrophic muscle changes [9–11,15,16]. In an epidemiologic study involving 2,586,830 inhabitants of north-east Italy, the recorded incidence rate of CMD for the period 1979 to 1993 was 4.65 in 100,000 [17]. The data indicate that this myopathy is among the most frequent neuromuscular diseases with autosomal recessive transmission.

Several CMD types are now known to be associated with abnormal glycosylation of α-dystroglycan. Protein *O*-mannosylation has been described in mammalian brain, in a ratio of 1:3 relative to the more common protein-bound GalNAc-1-*O*-Ser/Thr *O*-glycans [18]. However, only a limited number of glycoproteins of brain, peripheral nerve and skeletal muscle are known to be *O*-mannosylated [19]. Fig. 1 shows the major sialylated *O*-glycosidically linked oligosaccharide in α-dystroglycan from bovine peripheral nerve [19,20] and rabbit skeletal muscle [21]. The sialylα2,3Galβ1,4GlcNAc moiety of this sugar chain is required for interaction of α-dystroglycan with laminin [6,19,20]. *O*-mannosyl glycans are present in other mammalian glycoproteins and several different structures have been described (see [19] for references).

UDP-GlcNAc:α-3-D-mannoside β1,2-*N*-acetylglucosaminyltransferase 1 (GnT1, EC 2.4.1.101) [22,23] is the entry point for the conversion of oligomannose to hybrid and complex *N*-glycans. A TBLASTN screen of the Expressed Sequence Tag (EST) database for genes with significant sequence similarities to GnT1 showed the presence of human (Hs.183860) and mouse (Mm.2069) Unigenes encoding a protein similar to human GnT1 [24]. The human

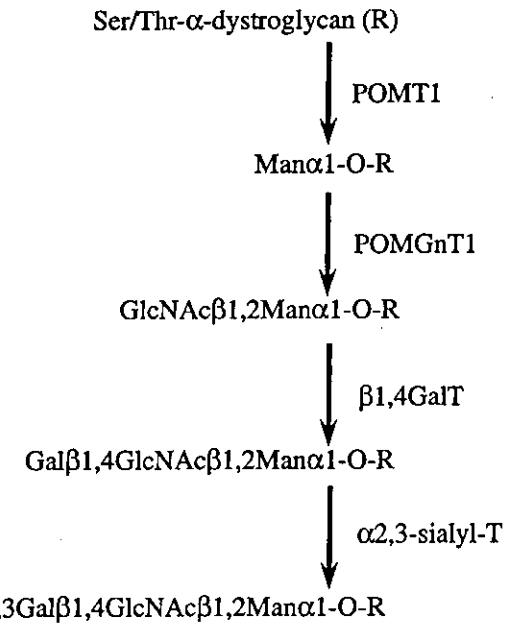

Fig. 1. The synthesis of the *O*-glycosidically linked tetrasaccharide of α-dystroglycan from bovine peripheral nerve and rabbit skeletal muscle. The first enzyme to act on the protein is POMT1 (Protein *O*-Mannosyltransferase 1) which adds a mannose residue (Man) to Ser and Thr residues of the protein. The gene encoding POMT1 is mutated in some cases of WWS. The next enzyme in the pathway is POMGnT1 (Protein *O*-Mannosyl β-1,2-*N*-acetylglucosaminyltransferase 1) which adds an *N*-acetylglucosamine residue (GlcNAc) in β1,2 linkage to the Man. The gene encoding POMGnT1 is defective in MEB disease. The next two enzymes, β1,4-galactosyltransferase (β1,4GalT) and α2,3-sialyltransferase (α2,3-sialyl-T), respectively add galactose (Gal) and sialic acid (sialyl) residues as indicated. No human disease has as yet been associated with these enzymes.

gene was cloned and expressed, and the recombinant protein was shown to incorporate GlcNAc from UDP-GlcNAc into several Manα1-O-R acceptors. The product formed with Manα1-O-benzyl was shown to be GlcNAcβ1,2 Manα1-O-benzyl and the enzyme was therefore named UDP-GlcNAc: α-D-mannoside β-1,2-*N*-acetylglucosaminyltransferase 1.2 (GnT1.2; gene *MGAT1.2*) [24]. GnT1.2 was appreciably more active with the *O*-mannosyl glycopeptide CYA{Manα1-O-T}AV (Km = ~ 12 mM) than with Manα1-O-benzyl (Km > 30 mM). Yoshida *et al.* [25] cloned and expressed the same human gene and showed that the recombinant enzyme incorporated GlcNAc into the *O*-mannosyl glycopeptide *N*-acetyl-AAP(Man-T)PVAAP-NH_2. However, they did not detect any enzyme activity with Manα1-O-R acceptors in which R was not a peptide, at least under their assay conditions. They named the enzyme Protein *O*-Mannosyl β-1,2-*N*-acetylglucosaminyltransferase 1 (POMGnT1) (Fig. 1).

Muscle-Eye-Brain disease (MEB, OMIM 253280; OMIM, Online Mendelian Inheritance in Man) was first described in 1978 [26]. MEB is an autosomal recessive disorder characterized by congenital muscular dystrophy, ocular abnormalities and cobblestone type brain malforma-